universität wien

MASTERARBEIT

Titel der Masterarbeit

„Bioactive compounds of Neurolaena lobata inhibit the translocated NPM/ALK gene“

verfasst von

Izabella Kiss, BSc

angestrebter akademischer Grad

Master of Science (MSc)

Wien, 2014

Studienkennzahl lt. Studienblatt:	A 066 834
Studienrichtung lt. Studienblatt:	Masterstudium Molekulare Biologie
Betreut von:	Ao. Univ. - Prof. Dr. Georg Krupitza

ABSTRACT

The oncogenic NPM/ALK chimera generated by the t(2;5)(p23;q35) chromosomal translocation promotes the proliferation and the survival of ALCLs (anaplastic large cell lymphomas). In search of a novel therapy for NPM/ALK positive ALCL the dichloromethane extract (DME) of the traditional healing plant *Neurolaena lobata* was shown to inhibit the NPM/ALK expression.

In this regard, active constituents of the extract grouped in *furanoheliangolides* and *germacranolides* sesquiterpene lactones were isolated. The group of *furanoheliangolides* consisting of the compounds Neurolenin A, B, C, D and Lobatin A and *germacranolides* subdivided in LobatinB, 8β-isovaleryloxy-9α-hydroxy-calyculatolide (OH-CAL), and 8β-isovaleryloxy-9α-acetoxy-calyculatolide (OAc-CAL) were tested for their anti-neoplastic properties in NPM/ALK positive ALCL and in leukaemia (HL-60) cell lines. Proliferation-, Cell-Titer Blue-, Apoptosis- assays as well as FACS-, Western blot- and q-PCR-analyses were conducted with sesquiterpene lactones treated cancer and normal (PBMCs) cells. Thereby, Lobatin B and Neurolenin B emerged as very active constituents against ALCL cells.

Lobatin B and Neurolenin B suppressed the expression of NPM/ALK, JunB and consequently PDGF-Rβ, arrested cells in G2/M phase resulting in ALCLs growth inhibition and induced apoptosis. Both compounds target malignant cells and thus, also HL-60 cell proliferation and mitochondrial activity were inhibited, whereas normal PBMCs were spared.

In conclusion, sesquiterpene lactones, especially Lobatin B and Neurolenin B may be considered for new therapeutic approaches for ALCLs.

ZUSAMMENFASSUNG

Das onkogene Chimärprodukt NPM/ALK, das durch die chromosomale t(2;5)(p23;q35) Translokation zustande kommt, treibt die Proliferation von anaplastischen groß-zelligen Lymphomen (ALCL) voran und sichert deren Überleben. Auf der Suche nach neuen Therapiemöglichkeiten für NPM/ALK positive ALCL wurde gezeigt, dass der Dichlormethanextrakt (DME) der traditionellen Heilpflanze *Neurolaena lobata* die NPM/ALK Expression inhibiert. Aufgrund dieser Erkenntnis wurden aktive Bestandteile des Extraktes, die in *Furanoheliangolide* und *Germacranolide* Sesquiterpene Lactone gegliedert wurden, isoliert. Die Gruppe der *Furanoheliangolide,* bestehend aus Neurolenin A, B, C, D und Lobatin A und die der *Germacranolide* unterteilt in LobatinB, 8β-isovaleryloxy-9α-hydroxy-calyculatolide (OH-CAL), und 8β-isovaleryloxy-9α-acetoxy-calyculatolide (OAc-CAL) wurden auf ihre anti-neoplastischen Eigenschaften in NPM/ALK positive ALCL und in Leukämie Zelllinien getestet und Proliferations-, FACS-, Western Blot- und qPCR-Analysen, sowie CellTiter Blue-, und Apoptose- Assays unterzogen. Dabei, erwiesen sich die Lactone, Lobatin B und Neurolenin B als sehr wirksame Substanzen gegen ALCL, wobei normale mononukleäre Zellen des peripheren Blutes (PBMCs) unbeeinträchtigt blieben. Lobatin B und Neurolenin B unterdrücken die Expression von NPM/ALK, JunB und infolgedessen auch PDGF-Rβ in ALCL Zelllinien. Außerdem führt eine solche Behandlung mit Lobatin B oder Neurolenin B zu einer Inhibierung des ALCL-Wachstums durch Arretieren der Zellen in der G2/M Phase und in Folge wird Apoptose ausgelöst. Die Ergebnisse lassen den Schluss zu, dass Lobatin B und Neurolenin B in Erwägung gezogen werden könnten, um neue Therapien gegen ALCL zu entwickeln.

Table of contents

ABBREVIATIONS

CD-417	murine NPM/ALK positive ALCL cell line
HL-60	human promyelocytic leukaemia cell line
SR-786	human NPM/ALK positive ALCL cell line
PBMC	peripheral blood mononuclear cells
ALL	acute lymphoblastic leukaemia
AML	acute myeloid leukaemia
ALCL	anaplastic large cell lymphoma
ALK	anaplastic lymphoma kinase
ATCC	American type culture collection
CLL	chronic lymphoblastic leukaemia
CML	chronic myeloid leukaemia
DMSO	dimethyl sulfoxide
DNA	deoxyribonucleic acid
DNAse	deoxyribonuclease
ECL	enhanced chemiluminescence
EDTA	ethylenediaminetetraacetic acid
FACS	fluorescence activated cell sorting
FCS	fetal calf serum

FDA	US Food and Drug Administration
G0, G1, G2	gap phases of the cell cycle
M-phase	mitosis
S-phase	DNA synthesis during cell cycle
NPM	nucleophosmin
p21	cyclin-dependent kinase inhibitor 1, tumour suppressor protein
PAGE	polyacrylamide gel electrophoresis
PARP	poly(ADP-ribose)polymerase
PBS	phosphate buffered saline
PIM	protease inhibitor mix
PMSF	phenylmethylsufonyl fluoride
PDGFR-β	platelet-derived growth factor β
RPMI	cell culture medium (Rosewell Park Memorial Institute)
SDS	sodium dodecyl sulfate
TBS	Tris buffered saline
WHO	World Health Organization
TNF	Tumour necrosis factor
LPS	Lipopolysaccharide
THP-1	Human acute monocytic leukaemia

INTRODUCTION

CANCER

One of the major causes of death in the world is cancer. In 2012, 14 million new cancer cases were estimated and 8.2 million cancer-related deaths occurred worldwide. **(www.who.int)** 90%-95% of all cancer cases attribute from lifestyle factors such as smoking, dieting, obesity, infections, radiation, stress, physical inactivity and environmental pollutants. Only 5–10% are caused by inherited genetic alterations.

Currently, more than 200 different human cancer types are known. Although each cancer exhibits unique features, all cancer types share common characteristics that define the transformation of normal cells to cancer cells. In **2011, Hanahan and Weinberg** presented ten characteristics for malignancies including self-sufficiency in growth signalling, resistance to inhibitory growth signals, evasion of apoptosis (programmed cell death), induction and sustainment of angiogenesis, limitless replicative potential, invasion of tissue and expansion to distant sites (metastasis), avoiding immune destruction, tumour-promoting inflammation, genome instability and mutation, and deregulating cellular energetics.

Figure 1. Hallmark of cancer: the next generation **(Hanahan and Weinberg, 2011)**

LEUKAEMIA

In 2012, leukaemia, a cancer that initiates from blood stem cells of the bone marrow but more often in the white blood cells, was the tenth most common cancer in the world. Leukaemia is characterised by an increasing number of white blood cells. This kind of cancer is firstly grouped in myelogenous and lymphocytic leukaemia, based on the blood cells from where they arrived. Furthermore, lymphoma is divided in acute (fast growing) and chronic (slow growing) leukaemia. Thus, four main types are distinguished: acute lymphoblastic leukaemia (ALL), acute myeloid leukaemia (AML), chronic lymphoblastic leukaemia (CLL), and chronic myeloid leukaemia (CML) **(www.cancerresearchuk.org; www.cancer.org)**.

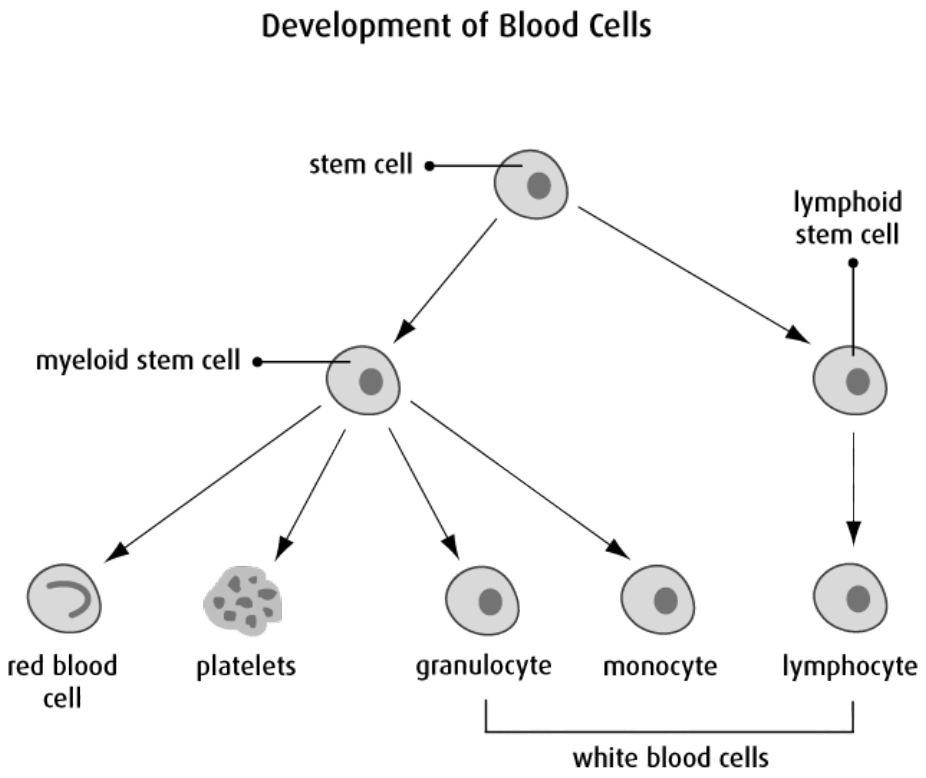

Figure 2. Development of blood cells (Taken from **http://www.cancer.ca**)

One of the main symptoms of leukaemia is anaemia, which occurs by a decrease of the red blood cells causing tiredness, breathlessness and paleness. Further symptoms are blood-clotting problems like easy bruising and bleeding from the gums due to low level of platelets. Serious infections are also common symptoms.

LYMPHOMA

One of the most common cancer types worldwide contributing 3,2% of the total number of new cancer cases in 2012 is Lymphoma **(www.wcrf.org)**.

Lymphoma occurs when lymphocytes, a type of white blood cell, divide faster or live longer than they are supposed to. Abnormal cells can spread to almost any body part through the lymphatic system. Malignant cells are often originating and expanding in the lymph nodes.

Lymphomas arising from non-lymphoid tissues such as skin, brain and bone are referred to as extranodal lymphomas. Lymphocytes including B-cells, T- cells and natural killer cells are part of the immune system and play an important role in fighting infections or diseases. Lymphoma is subdivided into non-Hodgkin lymphoma (NHL), which is marked by the presence of the Reed-Sternberg cell (giant cells), and Hodgkin lymphoma (HL).

Common symptoms for both variants of lymphoma include painless or sometimes painful swelling of lymph nodes, fever, unexplained weight loss and soaking night sweats. Other symptoms like weakness, fatigue, respiration troubles, itching as well as flulike symptoms are also associated with lymphoma **(www.lymphoma.org)**.

ALCL

ALCL (anaplastic large-cell lymphoma) is an aggressive and rare T-cell lymphoma **(Kadin et al., 1994)** comprising 10-20% of all NHL cases in children and 3% in adults **(Stein et al., 2000)**. In ALCLs an aberrant form of T-cell receptors (cytokine receptor CD30) is generated **(Stein et al., 1985)**.

WHO classification distinguishes between primary systemic ALK positive ALCL (ALK+ ALCL), primary systemic ALK negative ALCL (ALK- ALCL) and primary cutaneous ALCL. Systemic ALCL is associated with fevers, painless swelling of lymph nodes, rapid weight loss and tiredness **(www.lymphoma.org)**. A characteristic feature of cutaneous ALCL includes skin lesions that tend to ulcerate. ALK+ ALCLs occur more frequently in children and young adults, whereas ALK- ALCLs are more common in older patients (over age 60).

ALK- ALCL patients suffer more often from relapses by developed chemotherapy resistances, therefore ALK+ ALCL have better prognosis than ALK- ALCL. 60-80 % of ALK+ ALCLs can be cured by the standard chemotherapy CHOP (cyclophosphamide, doxorubicin, vincristine and prednisone) for T-cell lymphomas **(Savage et al., 2008)**.

NPM/ALK

ALK+ ALCLs are accompanied by chromosomal rearrangements of the anaplastic lymphoma kinase (ALK) gene, whereas in ALK- ALCLs ALK is in not expressed **(Savage et al., 2008)**. In ALK+ALCL, chimeric proteins are formed by a fusion of ALK to various partners. Fusion partners of ALK are in most cases NPM1 (nucleophosmin) and TPM3 (tropomysin 3), rarely TFG (TRCK fusion gene), ATIC and CLTCL, TPM4, MSN, ALO17, MYH9 **(www.atlasgeneticsoncology.org)**. 70-80% of all ALK+ cases contain the t(2;5)(p23;q35) translocation by which the oncogenic NPM/ALK (nucleophosmin /anaplastic lymphoma kinase) fusion protein is generated. **Morris et al. (1994)** discovered that the nucleophosmin gene, located on q35 region of chromosome 5 was fused to ALK gene on chromosome 2p23. In the resulting fusion protein, the amino terminus of nucleophosmin is linked to the catalytic domain of ALK **(Morris et al., 1994)** and ALK tyrosine kinase gets constitutively activated, thereby cell proliferation and survival increases **(Chiarle et al., 2003)**.

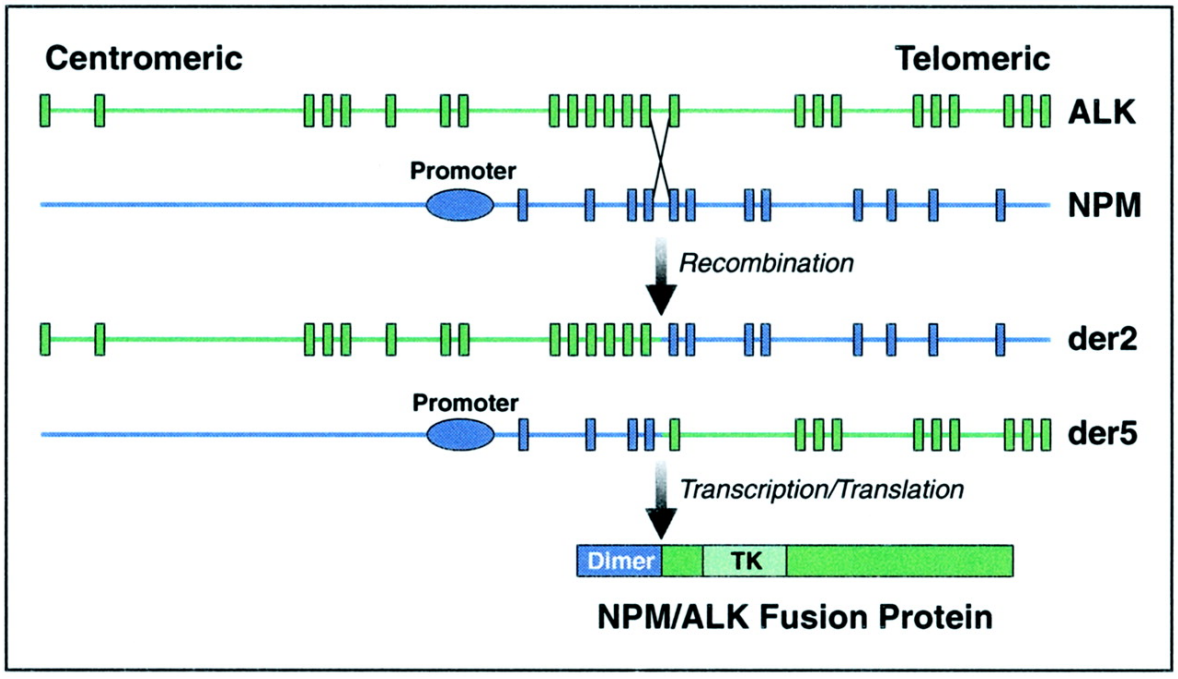

Figure 3. By NPM/ALK translocation a 80kDa oncogenic fusion protein containing a tyrosine kinase domain (TK) derived from ALK is generated **(www.jco.ascopubs.org)**.

Investigations are conducted to discover ~~a~~ treatment targeting ALK directly and small-molecule ALK inhibitors such as crizotinib (Xalkori, Pfizer) and NVP-TAE684 were described **(Hallberg and Palmer, 2011)**. In 2011, the U.S. Food and Drug Administration approved crizotinib to treat non-small-cell lung cancer (NSCLC) carrying the EML4-ALK translocation **(Gandhi et al., 2012)**. Presently, crizotinib is also being tested in clinical trials of ALCL. Studies demonstrated that NVP-TAE684 blocks the growth of ALK+ ALCL cell lines and suppresses lymphoma genesis in ALK+ ALCL mouse models **(Galkin et al., 2007)**. Imatinib, a tyrosine-kinase inhibitor, was shown to reduce ALK+ALCL growth and to alleviate the relapse rate by the recently discovered PDGFRB signal transductions cascade **(Laimer et al., 2012)**.

NATURAL PRODUCTS AS ANTICANCER AGENTS

Traditionally, plants were used for healing diseases including cancer. Therefore, it is understandable that natural sources play an important role for the development of new anticancer agents and more than 60% of the currently used anti-cancer agents are of plant origin **(Bhanot et al., 2011)**.

Vincristine

An example for a plant derived anticancer molecule in clinical use is vincristine (Oncovin), a vinca alkaloid from the plant *Catharanthus roseus* (Madagascar periwinkle). This plant enjoyed a good reputation in various parts of the world as home remedy **(Johnson et al., 1963)**. Plant extracts were used for treating or healing of haemorrhage, scurvy, toothache, wounds, diabetic ulcers and hyperglycaemia **(Gidding et al., 1999)**.

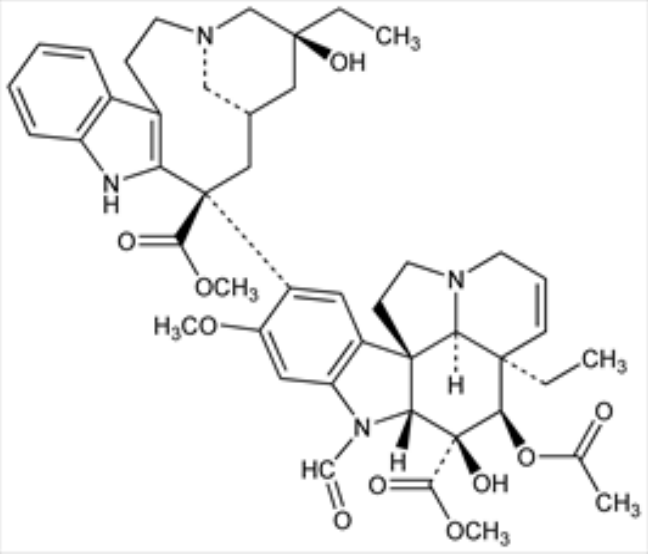

Figure 4. Structural formula of Vincristine **(www.medicinescomplete.com)**

Cytotoxic vincristine acts as a mitotic inhibitor by binding to the building block of tubulin, a protein that creates spindle fibres (microtubules). Thereby, microtubule formation is inhibited, followed by a cell division halt and apoptosis **(Gidding et al., 1999)**. Thus, vinca alkaloids successfully prevent cancer cells from multiplying.

Vincristine is administered intravenously as a component in combinatorial chemotherapy to treat non-Hodgkin-, Hodgkin lymphoma and neuroblastoma **(Gidding et al., 1999)**. Side effects like peripheral neuropathy, suppression of bone marrow activity, constipation, nervous system toxicity, nausea, and vomiting, are observed. In 1963 the US Food and Drug Administration (FDA) approved Vincristine **(www.fda.gov)**.

Etoposide

Another antineoplastic drug is etoposide, a semisynthetic derivative of podophyllotoxin found in *Podophyllum peltatum* (American Mayapple). Podophyllin-containing materials have been used as folk medicines for centuries **(Hande et al., 1998)**. Etoposide acts as a topoisomerase inhibitor by interfering with the action of topoisomerase enzymes, which are controlling the DNA structure during replication. Prevention of DNA religation by etopiside's blocking mechanism leads to breaks in DNA strands and thereby, apoptosis is promoted **(Pommier et al., 2010)**. Cancer cells rely on these topoisomerase enzymes more than normal cells due to faster cell division of malignant cells **(Gordaliza et al., 2004)**.

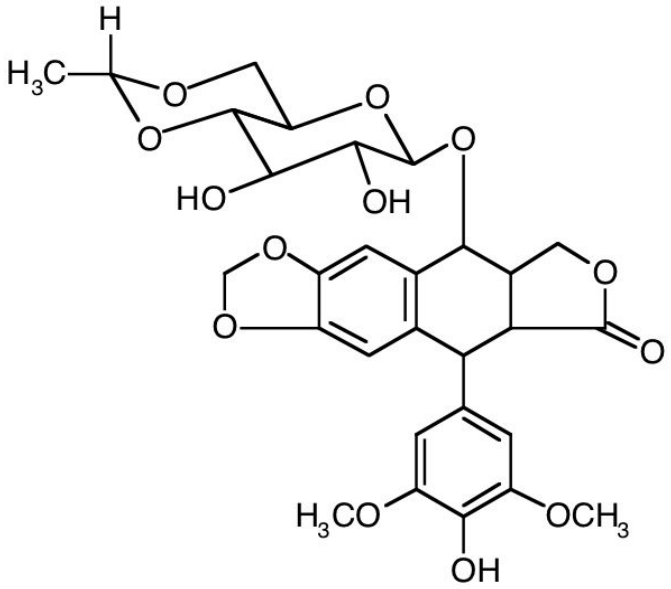

Figure 5. Structural formula of etoposide **(www.commons.wikimedia.org)**

Since 1983 the US Food and Drug Administration (FDA) approved etoposide, **(www.fda.gov)** it has been usually used as chemotherapeutic drug. Etoposide is intravenously or orally administered to combat sarcoma, lung cancer, testicular cancer, lymphoma, leukaemia and glioblastoma. Common side effects of etoposide are low blood pressure, hair loss, constipation or diarrhoea, dizziness, visual problems, paleness, fainting, nausea, vomiting, loss of appetite etc.

Neurolaena lobata

Neurolaena lobata, a herbaceous plant, distributed in Central America and in the Caribbean area is widely used as remedy to cure a variety of diseases **(Lajter et al., 2014; Passreiter et al., 1998)**. Leaves and roots of *N. lobata* were used for centuries to heal diseases. In traditional medicine the leaves are used to treat cancer, ulcers, inflammatory skin disorders and diabetes and moreover, to prevent parasitic ailments such as malaria, fungus, ringworm, and dysentery **(Lajter et al., 2014)**.

Since the sesquiterpene lactones, subdivided in *germacranolides* and *furanoheliangolides*, were identified to be responsible for different pharmacological activities of *N. lobata* **(Passreiter et al., 1998)**, methods for isolation of these compounds have been improved. For sesquiterpene lactones purification, an *N. lobata* extract was fractionated by column chromatography, identified by spectroscopic methods and finally quantified **(McKinnon et al., 2014)**. By now, sixteen sesquiterpene lactones of the *germacranolide* and *furanoheliangolide* type, *seco-germacranolide* sesquiterpene*s, epoxy-germacranolide* esters, and an *eudesmanolide* have been isolated from *N. lobata* **(Passreiter et al., 1995; Lajter et al., 2014)**.

The *germacranolides* include the compounds Neurolenin A, B, C, D, E, F and Lobatin A, whereby the group of *furanoheliangolides* consists of LobatinB, 8β-isovaleryloxy-9α-hydroxy-calyculatolide (OH-CAL), and 8β-isovaleryloxy-9α-acetoxy-calyculatolide (OAc-CAL) **(Passreiter et al., 1998)**. Furthermore, several flavonoids were described and some thymol derivatives were found in roots of *N. lobata* **(Passreiter et al., 1997)**.

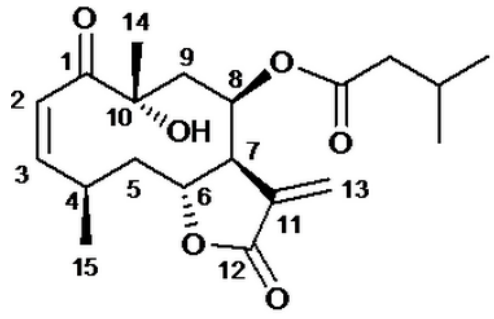

Lob 1

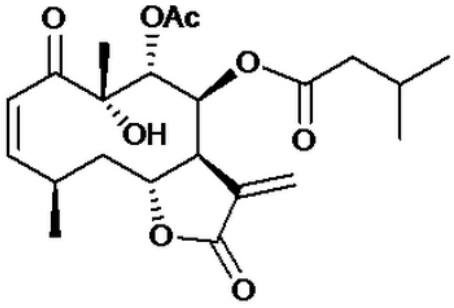

Lob 2

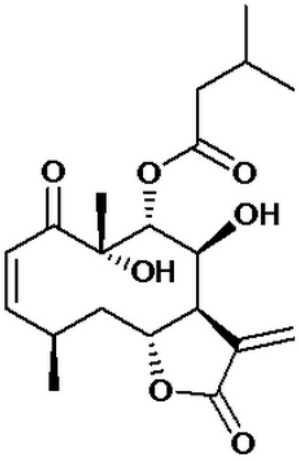

Lob 3

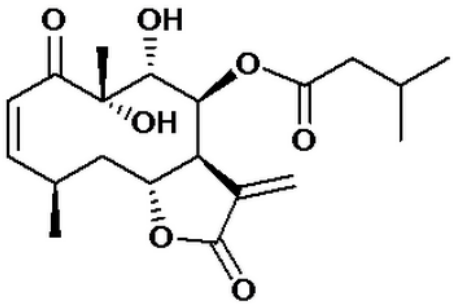

Lob 4

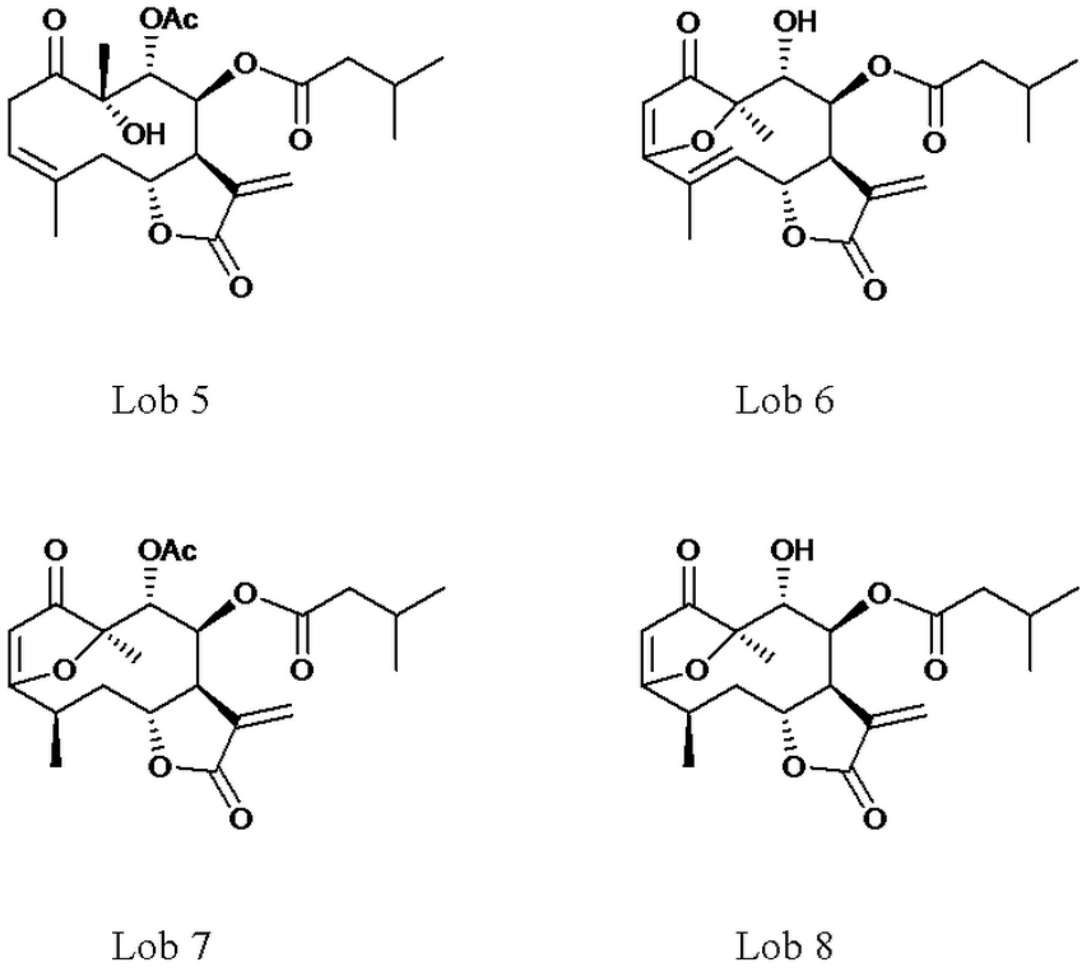

Figure 6. Structures of *germacranolide* and *furanoheliangolide* sesquiterpene lactones **(McKinnon et al., 2014)**

Germacranolides: Neurolenin A (Lob 1), Neurolenin B (Lob 2), Neurolenin C (Lob 3), Neurolenin D (Lob 4), Lobatin A (Lob 5)

Furanoheliangolides: Lobatin B (Lob 6), 8β-isovaleryloxy-9α-acetoxy-calyculatolide (Lob 7), 8β-isovaleryloxy-9α-hydroxy-calyculatolide (Lob 8)

Several studies approved the anti-parasitic and anti-cancer properties of *N. lobata* sesquiterpene lactones. *Germacranolide* and *furanoheliangolide* type of *N. lobata* were shown to be active against malaria pathogen, *Plasmodium falciparum* **(François et al., 1996)**. Furthermore, isolated sesquiterpene lactones showed anti-proliferative effects against four human cancer cell lines (A2780, A431, HeLa, and MCF7) **(Lajter et al., 2014)** as well as cytotoxity on human carcinoma cell lines (GLC4 and COLO 320 tumour cell lines) were discovered **(François et al., 1996)**. Some studies confirmed as well the *in vitro* anti-neoplastic, anti-protozoal and anti-inflammatory activity of the *N. lobata* compounds and extracts, and others reported anti-feedant and anti-viral potential **(Bedoya et al., 2008; Berger et al., 2001; Passreiter et al., 1997; Unger et al., 2013; Walsche-Roussel et al., 2013)**. In former studies the *furanoheliangolide* Lobatin B and the *germacranolide* Neurolenin B emerged as very active compounds against human cancer cell lines **(Lajter et al., 2014; François et al., 1996)**. Investigations revealed that the isolated *germacranolides* Neurolenin B and the *furanoheliangolide* Lobatin B reduce the LPS-stimulated TNF-α production in THP-1 monocytes **(Walsche-Roussel et al., 2013)** and downregulate the expression of E-selectin on LPS- and TNF-α-stimulated endothelial cells **(McKinnon et al., 2014)**.

AIM

Previous studies demonstrated that the dichloromethane extract of *N. lobata* inhibited ALK+ ALCL proliferation, induced tumour suppressors, down-regulated various oncogenes and triggered apoptosis **(Unger et al., 2013)**. In continuation of **Unger's work (2013)**, investigations were conducted to identify effective compounds among the eight isolated *germacranolide* and *furanoheliangolide* sesquiterpene lactones of the ethno-pharmacological plant *N. lobata* against lymphomas. Therefore, detailed examinations on anti-neoplastic activities of sesquiterpene lactones were carried out in acute promyelocytic HL-60 cells, which presents a subtype of AML and in human (SR-786) and murine (CD-417) ALK+ALCL cell lines. The *germacranolides* are represented by Neurolenin A, B, C, D and Lobatin A, whereas LobatinB, 8β-isovaleryloxy-9α-hydroxy-calyculatolide (OH-CAL), and 8β-isovaleryloxy-9α-acetoxy-calyculatolide (OAc-CAL) presents the group of *furanoheliangolides*.

In this present work the sesquiterpene lactones were also tested on isolated PBMC´s to evaluate the specificity of *N. lobata* compounds towards neoplastic cells. Additionally, the impact of the specific ALK-inhibitor TAE-684 on ALCLs and NPM/ALK negative cells was examined to find out whether an ALK-inhibitor acts similar to sesquiterpene lactones.

RESULTS

Furanoheliangolide sesquiterpene lactones

Anti-proliferative effects of *N. lobata furanoheliangolide* sesquiterpene lactones in ALCL cells

In order to explore the effects of isolated *N. lobata* compounds (**Fig. 7a**) on cell growth of ALK- positive ALCL, murine CD-417 (**Fig. 7b**) and human SR-786 cells (**Fig. 7c**) were treated with 1 µM and 3 µM Lobatin B, 8β-isovaleryloxy-9α-hydroxy-calyculatolide (OH-CAL), and 8β-isovaleryloxy-9α-acetoxy-calyculatolide (OAc-CAL), whereby, only 3 µM Lobatin B inhibited proliferation of murine CD-417 cells and eradicated them after 24 h. Human SR-786 cell growth was inhibited by 1 µM Lobatin B. 3 µM OAc-CAL slightly inhibited SR-786 cell growth after 24 h whereas OH-CAL did not inhibit growth of both cell lines. Hence, further experiments were performed with Lobatin B to characterise the cytotoxic mechanisms and compared to OH-CAL. Interestingly, OH-CAL and OAc-CAL slightly but consistently induced the growth of CD-417 cells after 16 h of treatment.

a

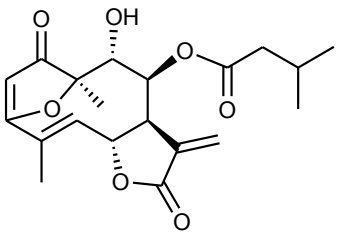

Lobatin B

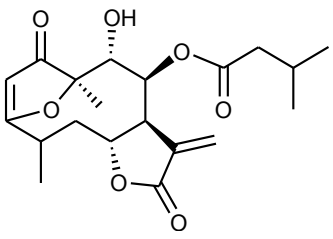

OH-CAL

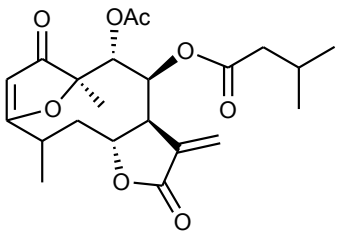

OAc-CAL

b

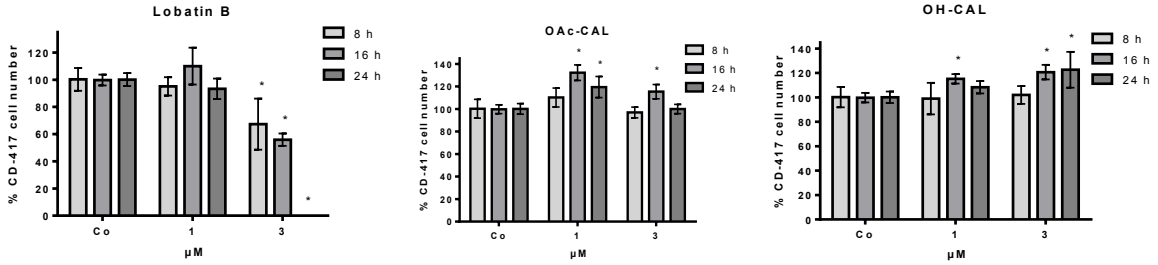

c

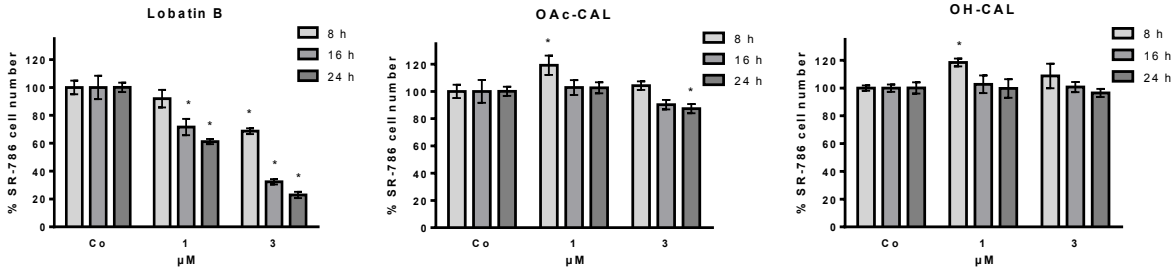

Figure 7. Anti-proliferative effects of (a) *N. lobata* compounds in (b) murine CD-417 and (c) human SR-786 cells. After 8, 16 and 24 h of treatment with 1 µM and 3 µM of Lobatin B, 8β-isovaleryloxy-9α-hydroxy-calyculatolide (OH-CAL), and 8β-isovaleryloxy-9α-acetoxy-calyculatolide (OAc-CAL) cells were counted by using a Casy cell counter. The relative cell number is presented as percent of control. Experiments were performed in triplicate, error bars indicate means +/- SD, and asterisks significance ($p<0.05$; t-test).

Mitochondrial activity and cell cycle distribution upon Lobatin B and OH-CAL treatment

The mitochondrial metabolism of SR-786 cells, which was measured by CellTiter-Blue assay, was only weakly affected by Lobatin B and OH-CAL (**Fig. 8a**). The weak inhibition of mitochondrial activity was in obvious contrast to the strong inhibition of cell proliferation (**Fig. 8b**). This evidenced that growth inhibition was not due to a general toxicity that was imposed on mitochondrial function but supposedly to a more specific anti-proliferative activity. Next, the effect of Lobatin B on SR-786 the distribution of cells within the cell cycle was evaluated by flow cytometric analysis (FACS). Treatment with 3 µM Lobatin B for 8 h caused the accumulation of SR-786 cells in G2/M phase at the expense of cells in G1 (**Fig. 8b**). Therefore, SR-786 were still able to pass through S-phase, because no accumulation of S-phase cells was observed and Lobatin B inhibited proliferation by arresting SR-786 cells in G2/M. OH-CAL treatment had no effect on cell cycle distribution.

a b

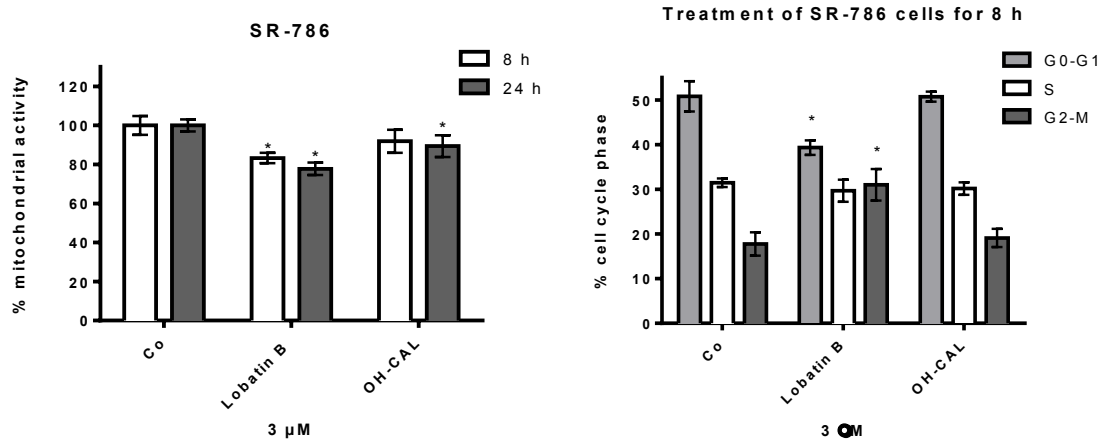

Figure 8. Potential mechanisms of proliferation inhibition by Lobatin B in SR-786 cells. (a) Cells were treated with 3 µM Lobatin B and OH-CAL for 8 h and 24 h when CellTiter-Blue reagent was added and measured at 570 nm using a multi-well plate reader. (b) Cell cycle distribution upon treatment with Lobatin B and OH-CAL. SR-786 cells were incubated with 3 µM of each compound for 8 h and then subjected to FACS analysis. Experiments were performed in triplicate, error bars indicate means +/- SD, and asterisks significance ($p<0.05$; t-test).

Lobatin B inhibits NPM/ALK expression in SR-786 cells

In ALCL cells the NPM/ALK chimera is driving proliferation. Therefore, it was tested whether Lobatin B affected the expression of NPM/ALK. Lobatin B treatment strongly suppressed the level of the NPM/ALK after 8 h and 24 h, whereas OH-CAL affected NPM/ALK expression only marginally after 24 h (**Fig. 9a,b**). Thus, Lobatin B specifically abrogated the expression of NPM/ALK and this was most likely causal for growth inhibition of SR-786 cells. Interestingly, Lobatin B caused a fluctuation of nucleophosmin and also OH-CAL suppressed nucleophosmin expression after 24 h.

To investigate at which stage the expression of NPM/ALK became down-regulated by Lobatin B, the transcript levels were analysed. NPM/ALK- and also nucleophosmin mRNAs became reduced upon Lobatin B treatment (**Fig. 10a,b**), hence giving a clue as to how Lobatin B mediated the regulation of NPM/ALK, i.e. by interfering with a factor or a site regulating nucleophosmin transcription. The fact that nucleophosmin protein level remained high upon Lobatin B treatment might have been due to high stability of the polypeptide. Yet, there was still a discrepancy because “inactive” OH-CAL treatment destabilised the protein expression of nucleophosmin and slightly that of NPM/ALK after 24 h. Therefore, the way of transcriptional regulation of NPM/ALK by Lobatin B has to be substantiated by future investigations.

The transcription of the JunB proto-oncogene was shown to be regulated by NPM/ALK **(Laimer et al., 2012; Staber et al., 2007)** and accordingly Lobatin B treatment suppressed JunB mRNA levels (**Fig. 10c**). The Jun family of transcription factors are components of the AP-1 transcription factor complex and AP-1 (activator protein 1) is involved in cell proliferation and apoptosis (**Pearson et al., 2011**), which provides a mechanistic link between Lobatin B treatment, the down-regulation of NPM/ALK and subsequently of JunB, and the inhibition of cell proliferation/induction of apoptosis.

a b

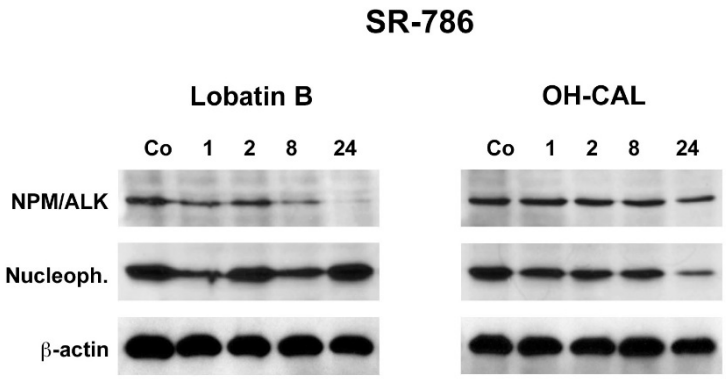

Figure 9. Lobatin B downregulates NPM/ALK expression in SR-786. Cells were treated with 3 µM Lobatin B (a) and 8β-isovaleryloxy-9α-hydroxy-calyculatolide (OH-CAL; b) for 1, 2, 8, and 24 h, harvested and subjected to Western blot analysis using the indicated antibodies. β-actin expression served as control for equal sample loading.

a b c

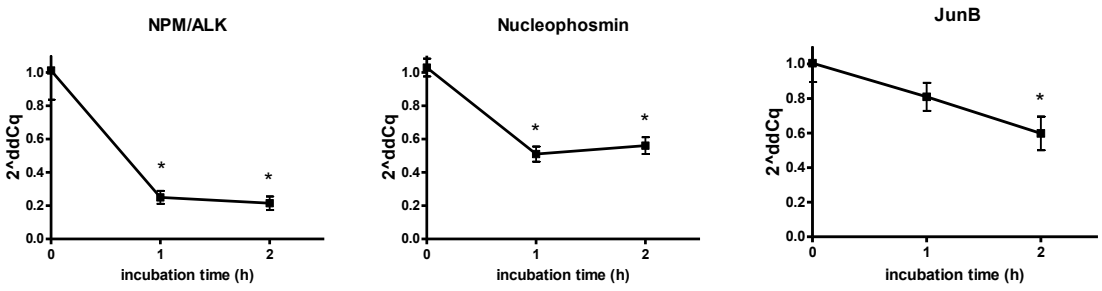

Figure 10. Quantitative PCR analysis. SR-786 cells were treated with 3 µM Lobatin B for the indicated times and the mRNA expression of NPM/ALK (a), nucleophosmin (b), and JunB (c) measured and normalized to GAPDH mRNA. Experiments were performed in triplicate, error bars indicate means +/- SD, and asterisks significance ($p<0.05$; t-test).

Lobatin B affects expression of Jun family members and induces tumour suppressor p21

The expression of the Jun family was further analysed at the protein level. JunB is the main transcription factor in the AP-1 complex induced by NPM/ALK **(Mathas et al., 2002; Staber et al., 2007)** and Lobatin B treatment inhibited the expression of JunB protein (**Fig. 11a**), which is consistent with suppression of its mRNA. Lobatin B induced c-Jun, which was strictly accompanied by an induction of p21. It was shown that c-Jun together with the ubiquitous transcription factor SP1 transactivates p21 expression **(Kardassis et al., 1999)**. On the other hand, also silencing of c-Jun by siRNA caused the upregulation of p21 and accumulation of NPM/ALK positive ALCL cells in G2/M at expense of S-phase cells (**Leventaki et al., 2007**). Therefore, both scenarios c-Jun induction and c-Jun inhibition may cause p21-mediated G2/M arrest. In contrast to the observations of **Leventaki et al. (2007)** describing that c-Jun down-regulation being accompanied by a loss of S-phase cells, we here report that upregulation of c-Jun was accompanied by a loss of G1-phase cells.

Lobatin B enhanced c-Jun similar to treatment with the DME of *N. lobata* **(Unger et al., 2013)**. However, the regulation of c-Jun by Lobatin B remained unclear. Since c-Jun can substitute for JunB the upregulation of c-Jun might be part of a compensatory feed back loop in response to JunB inhibition. Interestingly, JunD levels fluctuated upon Lobatin B treatment similar to the observed nucleophosmin fluctuations.

OH-CAL induced neither c-Jun nor p21 (**Fig. 11b**) and transiently suppressed JunB independent of NPM/ALK, because NPM/ALK remained expressed at the time point when JunB decreased. It is however possible that the activity of NPM/ALK became compromised, which we did not monitor. This short downregulation was not substantial and had no effect on the cell cycle. Jun family members, especially JunB promotes ALCL development through transcriptional activation of PDGFR-ß as shown in an ALCL mouse model (**Laimer et al., 2012**). In the human SR-786 ALCL cell line PDGFR-ß is not expressed.

Therefore, murine CD-417 ALCL cell line was used to test the effect of Lobatin B on PDGFR-ß expression. Lobatin B treatment first inhibited NPM/ALK (2h) and subsequently JunB and PDGFR-β became downregulated (**Fig. 11c**). Hence, Lobatin B inhibited the recently discovered NPM/ALK signal transduction cascade down to JunB and PDGFR-ß **(Laimer et al., 2012)**. As in SR-786 cells, Lobatin B induced c-Jun also in CD-417 cells.

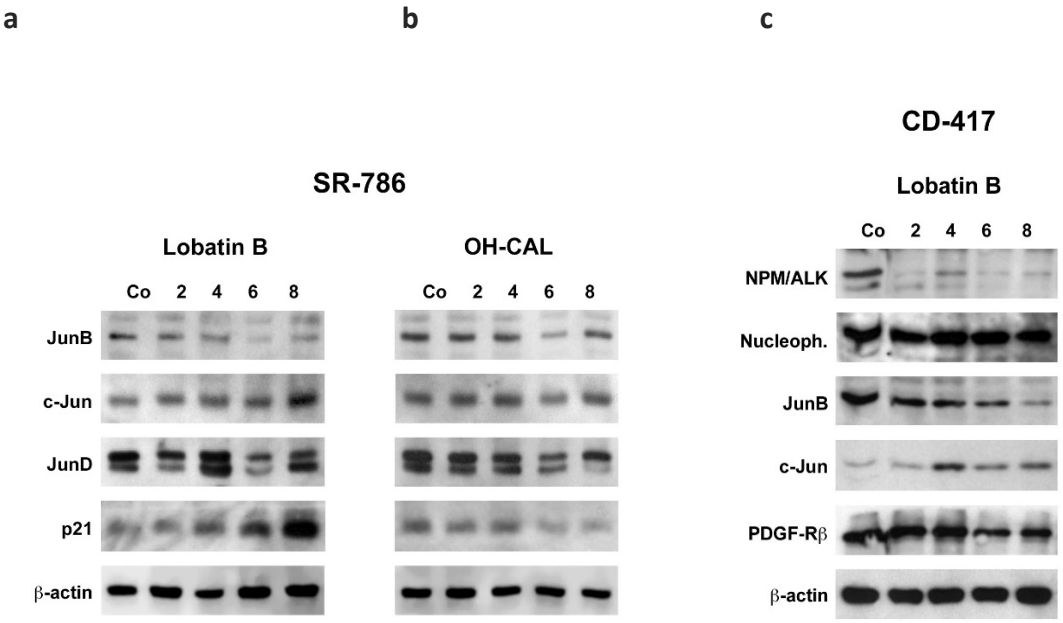

Figure 11. Effects of Lobatin B and OH-CAL on Jun-family members, PDGFR-ß and p21 in ALK-positive ALCL cells. SR-786 cells were treated with 3 µM Lobatin B (a) and 8β-isovaleryloxy-9α-hydroxy-calyculatolide (OH-CAL) (b) for 2, 4, 6, and 8 h, and CD-417 cells (c) were treated with Lobatin B. Then, cells were harvested and subjected to Western blot analysis using the indicated antibodies. β-actin expression served as control for equal sample loading.

Lobatin B triggers SR-786 cell death

Lobatin B induced cell death and significantly more apoptotic than necrotic cells were counted by HO/PI staining (**Fig. 12a**). This was confirmed by an induction of Caspase 3/7 activity within 16 h Lobatin B treatment and which decreased thereafter (**Fig. 12b**). Furthermore, caspase 3 activation was evidenced by its proteolytic degradation after 24 h and concomitant signature-type cleavage of its target PARP (**Fig. 12c**). OH-CAL treatment had some effect on caspase 3 pre-activation. Apparently this was owed to the rather similar structures of Lobatin B and OH-CAL. However, OH-CAL treatment did not seriously affect the survival mechanisms of SR-786 cells.

a

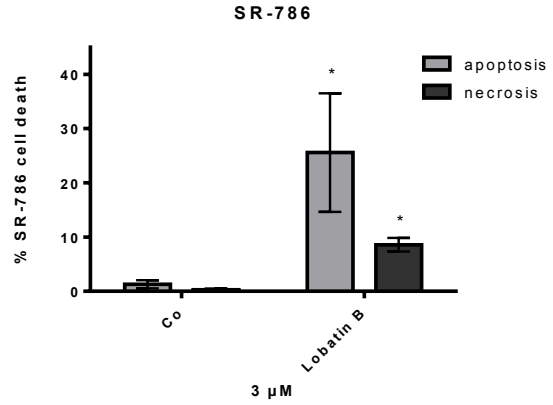

b

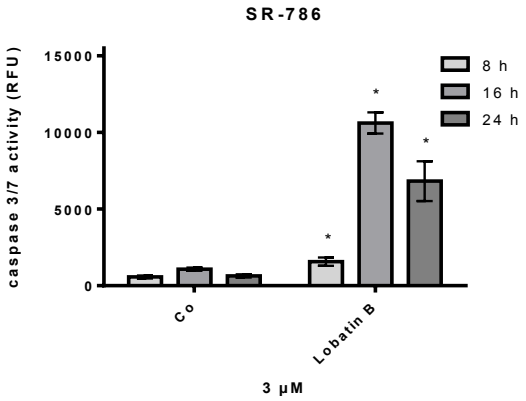

c

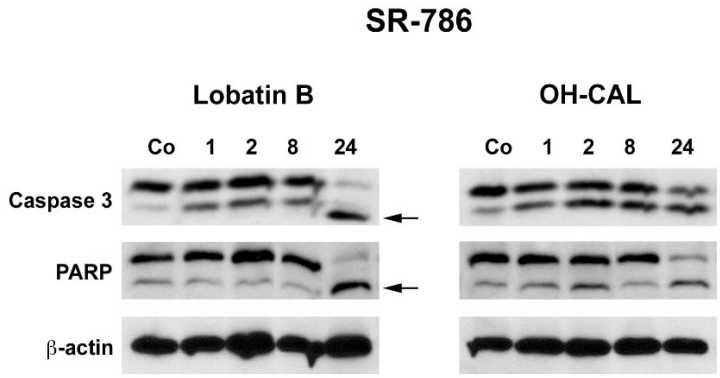

Figure 12. Apoptotic/necrotic cell death of SR-786 cells treated with *N. lobata* compounds. Cells were treated with 3 µM Lobatin B and after 24 h cell death was measured by (a) HO/PI staining, which enables the identification of apoptotic and necrotic cells. (b) Cells were treated with 3 µM of Lobatin B and after 8, 16 and 24 h ApoOne reagent was added and caspase 3/7 activity was measured. Experiments were performed in triplicate, error bars indicate means +/- SD, and asterisks significance ($p<0.05$; t-test). (c) Cells were treated with 3 µM Lobatin B (left panel) and 8β-isovaleryloxy-9α-hydroxy-calyculatolide OH-CAL (right panel) for 1, 2, 8, and 24 h, harvested and subjected to Western blot analysis using the indicated antibodies. β-actin expression served as control for equal sample loading.

Impact of Lobatin B on NPM/ALK negative cell types

To asses the specificity of Lobatin B towards lymphoma cells PBMCs from a healthy volunteer were treated with 3 µM Lobatin and OH-CAL. Interestingly, the number of PBMCs increased after 8 h of Lobatin B- and OH-CAL treatment (**Fig. 13a**) and this was accompanied by an increased mitochondrial activity (**Fig. 13b**). Then, PBMC numbers returned to control levels after 24 h and 48 h indicating that the initially propagating cell mass was finally subjected to a reduction process, which was paralleled by a significantly reduced mitochondrial metabolism upon Lobatin B treatment for 24 h. Since OH-CAL did not increase the metabolic activity after 8 h, the observed correlation between PBMC number and their mitochondrial activity (also by Lobatin B treatment) was coincidental.

Furthermore, HL60 leukaemia cells, which do not harbour the NPM/ALK translocation, were tested to study the specificity of Lobatin B towards NPM/ALK. HL60 cell number was reduced by ~60% upon Lobatin B treatment (**Fig. 13a**), which severely inhibited also HL60 mitochondrial metabolism (**Fig. 13b**). This evidenced that Lobatin B exhibited additional effects beyond NPM/ALK inhibition targeting leukaemia cells but not PBMCs. Hence, the anti-proliferative effects of Lobatin B were specific for neoplastic cells (i.e. lymphoma and leukaemia cells), but with a higher specificity to those cells harbouring the NPM/ALK translocation, because SR-786 cells and CD417 cells were more sensitive towards Lobatin B than HL60 cells.

a

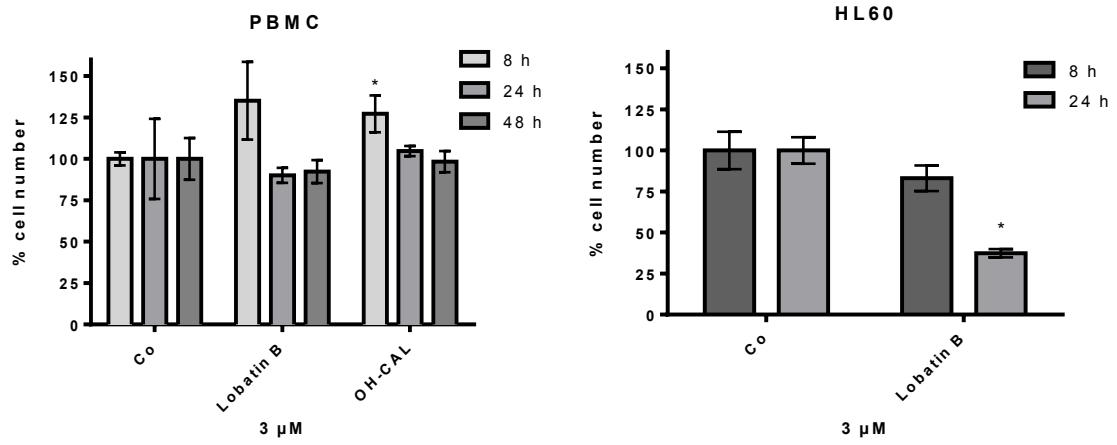

b

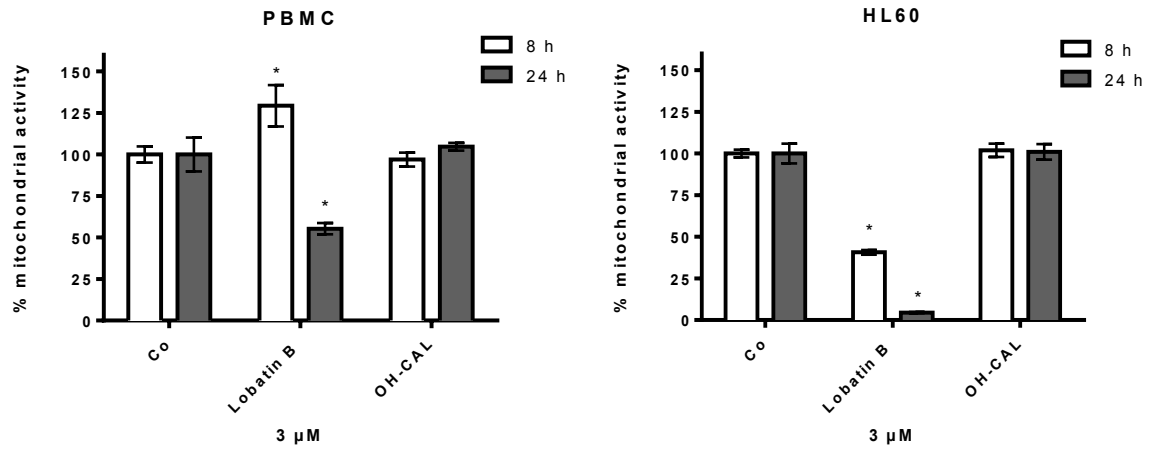

Figure 13. Treatment of PBMC and HL60 cells with *N. lobata* compounds. (a) Effects on cell number after treatment of PBMCs and HL60 cells with 3 µM Lobatin B and 8β-isovaleryloxy-9α-hydroxy-calyculatolide (OH-CAL) for 8 h, 24 h and 48 h. Cell number was measured by Casy cell counter. (b) PBMCs and HL60 cells were treated with 3 µM *N. lobata* compounds and after 8 h and 24 h of incubation with Lobatin B and OH-CAL CellTiter-Blue reagent was added and measured at 570 nm. Experiments were performed in triplicate, error bars indicate means +/- SD, and asterisks significance ($p<0.05$; t-test).

Specificity of the ALK inhibitor TAE-684

To estimate the impact of NPM/ALK on cell proliferation and the specificity of Lobatin B towards this mechanism SR-786 ALCL cells, ALK-negative HL60 cells, and normal PBMCs were treated with the specific NPM/ALK inhibitor TAE-684 **(Galkin et al., 2007)** and the effect on cell growth was compared. TAE-786 dose dependently inhibited the proliferation of SR-786 cells but not that of HL60 and PBMCs (**Fig. 14a**). Hence, NPM/ALK is driving proliferation and TAE-684 is more specific than Lobatin B regarding its property to target solely ALK. TAE-684 did not reduce the mitochondrial activity of HL60 cells but inhibited PBMC- and SR-786 mitochondrial metabolism (**Fig. 14b**). Obviously, mitochondrial activities did not correlate with cell growth rates and were therefore, independent of each other.

a

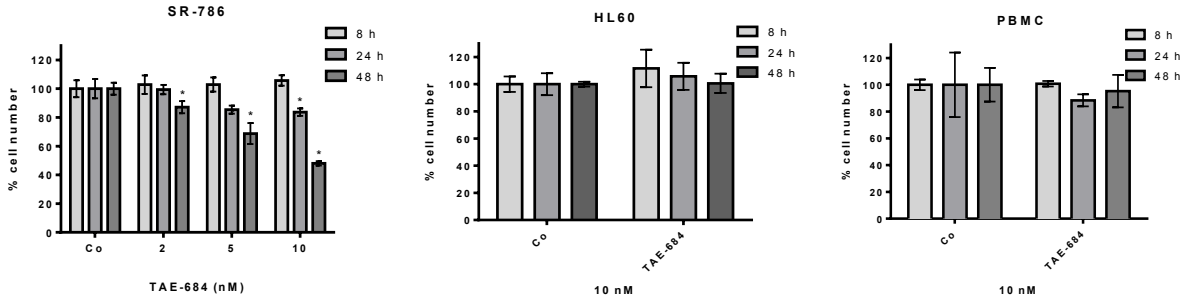

b

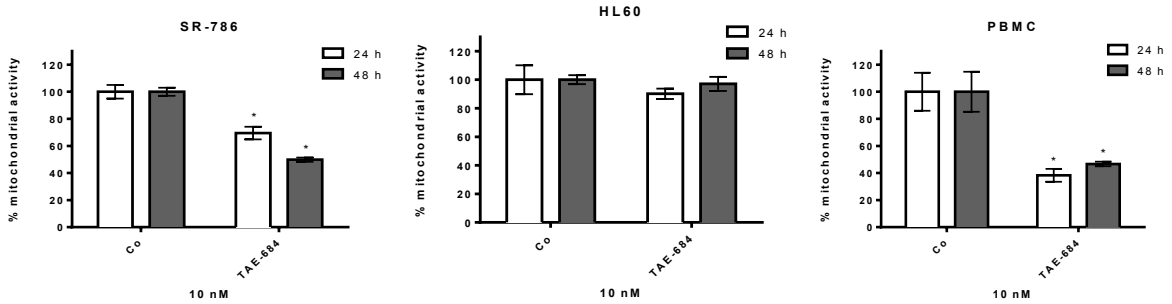

Figure 14. (a) Anti-proliferative effects of TAE-684 on SR-786-, HL60 cells and on PBMCs. Cells were treated with the indicated TAE-684 concentrations for 8 h, 24 h and 48 h and then counted by Casy. (b) Effect of TAE-684 treatment on SR-786-, HL60 cells, and PBMCs mitochondrial activity. Cells were treated with 10 nM TAE-684 for 24 h and 48 h and then, CellTiter-Blue reagent was added and measured at 570 nm. Experiments were performed in triplicate, error bars indicate means +/- SD, and asterisks significance ($p<0.05$; t-test).

Germacranolide sesquiterpene lactones

Anti-proliferative effects of *N. lobata germacranolide* sesquiterpene lactones

ALK- positive ALCL cells were treated with 1 µM and 3 µM of Lobatin A, Neurolenin A, B, C and D (**Fig. 15a**), and the proliferation of human SR-786- (**Fig. 15b**) and murine CD-417 cells (**Fig. 15c**) was examined. Neurolenin B inhibited the growth of both cell lines effectively in a dose and time depended manner, whereby murine CD-417 cells responded more sensitive to 3 µM Neurolenin B treatment than human SR-786 cells. 3 µM Neurolenin C and D treatment inhibited cell proliferation only weakly. Hence, further investigations were conducted with Neurolenin B and compared it with the closely related but least active compound, Neurolenin A.

a

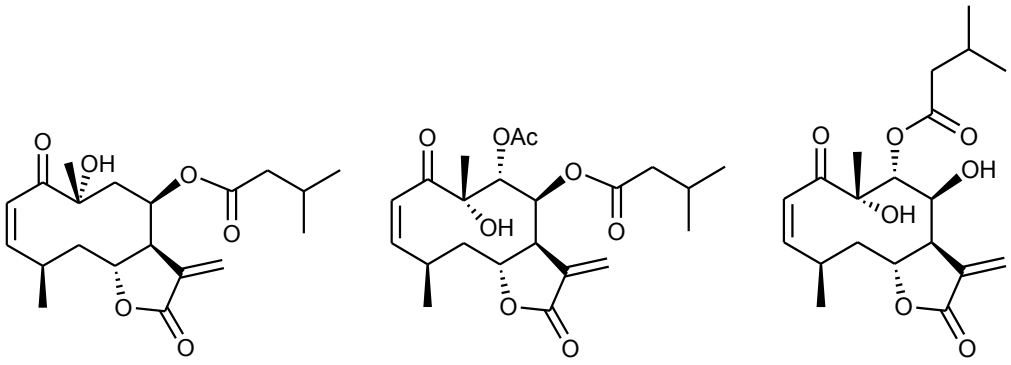

Neurolenin A Neurolenin B Neurolenin C

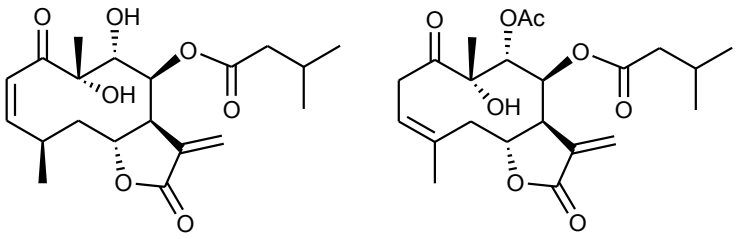

Neurolenin D Lobatin A

b

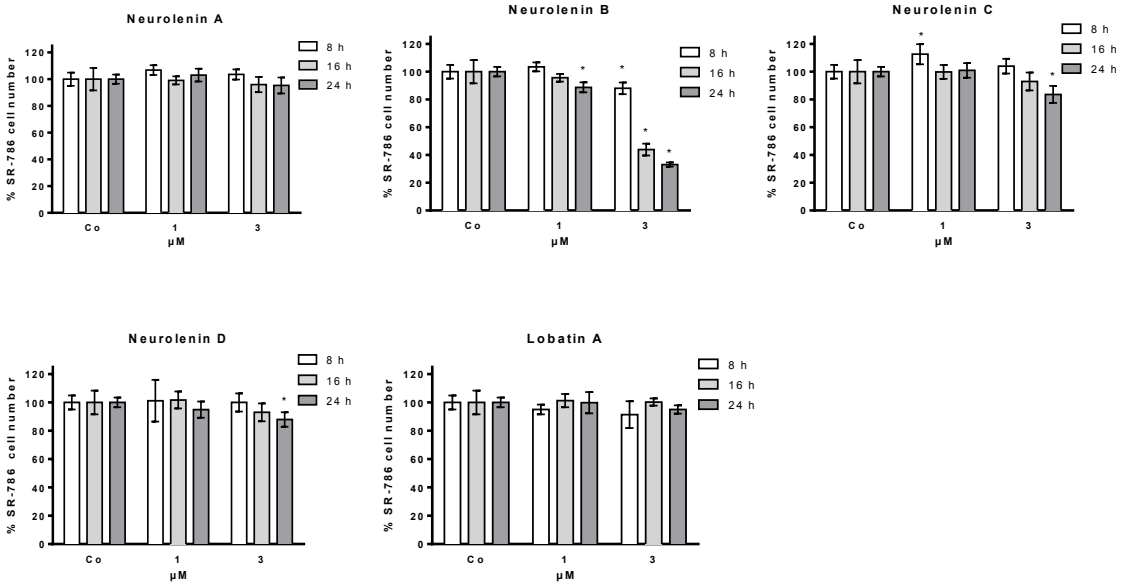

c

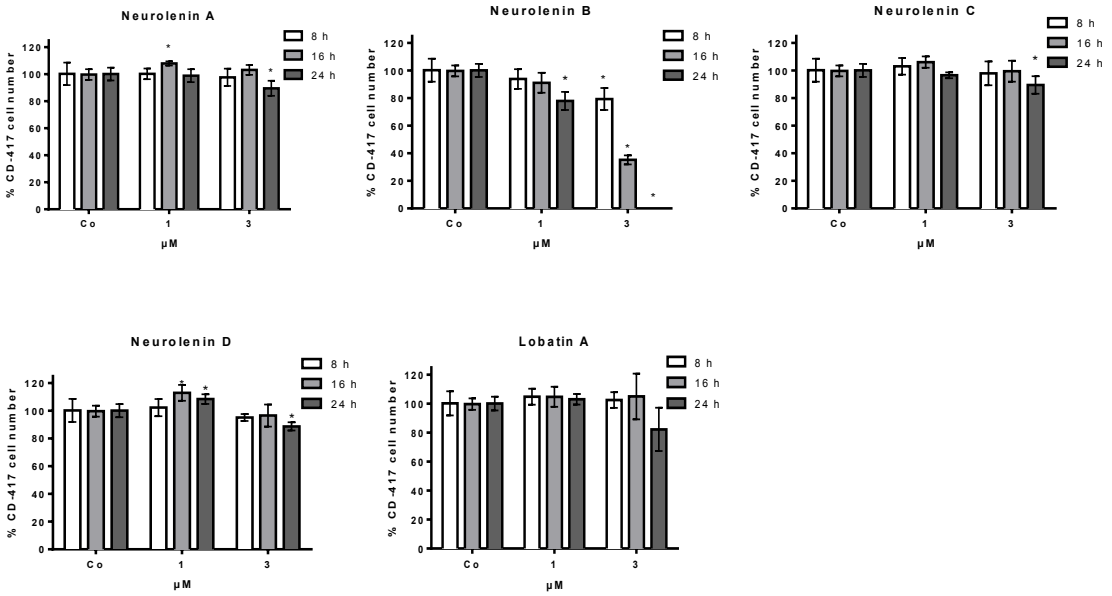

Figure 15. Impact of *Neurolaena lobata* compounds (a) on proliferation of human SR-786 (b) and murine CD-417 (c) cells. Cells were treated with 1 µM and 3 µM of Neurolenin A, B, C, D and Lobatin A and after 8, 16 and 24 h of incubation cells were counted using a Casy cell counter. The relative cell number is shown as percent of control. Experiments were performed in triplicate, error bars indicate means +/- SD, and asterisks significance ($p<0.05$; t-test).

Mitochondrial activity and cell cycle distribution upon Neurolenin A and B treatment

CellTiter-Blue assay was performed to evaluate the effect of Neurolenin B treatment on mitochondrial metabolism. The mitochondrial activity of SR-786 cells was weakly but significantly inhibited by 3 µM Neurolenin B, and interestingly, also by Neurolenin A (Fig. 16a). Treatment of SR-786 cells with 3 µM Neurolenin B for 8 h caused their accumulation in G2/M phase to the detriment of G1 cells as evidenced by FACS analysis (Fig. 16b). The decreased G1 fraction together with an increased cell number in G2/M implicated that cells maintained their capability to pass through S-phase despite Neurolenin B treatment, whereas G2/M passage was arrested. Consequently, Neurolenin B treatment blocked the cell cycle of ALK-positive ALCL in G2/M. Neurolenin A treatment showed no effect on cell cycle distribution. The effects on mitochondrial metabolism by Neurolenin A and B correlated neither with cell cycle alterations nor with the inhibition of cell proliferation.

a b

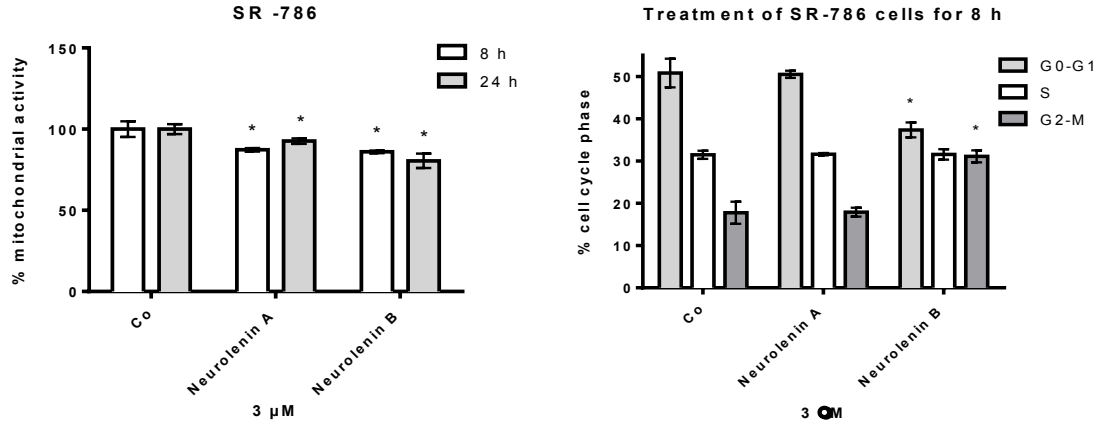

Figure 16. Analysis of mitochondrial activity and cell cycle progression upon Neurolenin A and B treatment in SR-786. (a) Cells were treated with 3 µM Neurolenin A and B and for 8h and 24 h when CellTiter-Blue reagent was added. Metabolic active cells were detected at 570 nm using a multi-well plate reader. The relative cell number is presented as percent of control. (b) Cells were harvested after 8 h of incubation with 3 µM Neurolenin A and B. Then, cells were fixed, stained and analysed by FACS for DNA content. Experiments were performed in triplicate, error bars indicate means +/- SD, and asterisks significance ($p<0.05$; t-test).

Neurolenin B modulates the expression of regulators of ALK+ALCL proliferation

It is widely accepted that the ALK translocation in ALCL cells causes enhanced proliferation and renders cells insensitive to death signals and therefore, causes the expansion of the ALCL population. Hence, blocking the signalling cascade triggered by NPM/ALK is considered as a target for therapeutic intervention. To study whether Neurolenin B treatment affected the expression of the NPM/ALK chimera Western blot analysis was performed. Neurolenin B treatment caused a severe down-regulation of NPM/ALK in human SR-786 cells after 8 h (**Fig. 17a**), whereas in murine CD-417 cells NPM/ALK expression became inhibited already after 4 h (**Fig. 17b**). Previous studies have shown that JunB expression was regulated by NPM/ALK **(Laimer et al., 2012; Staber et al., 2007)** and therefore, the expression of the Jun family upon Neurolenin A and B treatment was analysed. JunB levels were downregulated in SR-786-, and in CD-417 cells, by Neurolenin B (after 24 h and 8 h, respectively), JunD became suppressed by Neurolenin A and B after 24 h, and c-Jun by Neurolenin A after 24 h, although Neurolenin A had no significant effect on ALCL growth. This indicated that only JunB was forcing ALCL cells to replicate **(Staber et al., 2007)**, which is in agreement with the fact that JunB is the major component of the AP-1 complex in ALCL cells **(Mathas et al., 2002)**. Unlike Neurolenin A, Neurolenin B enhanced c-Jun expression without rescuing the cells from the oncolytic effects of this compound. To the contrary, c-Jun expression correlated with p21 up-regulation. It was shown that c-Jun together with SP1 transactivates p21 expression (**Kardassis et al., 1999**) and we demonstrated that increased p21 expression directly correlated with c-jun expression upon treatment with Neurolenin B or Lobatin B and the DME of *N. lobata* **(Unger et al., 2013; Kiss et al., in preparation)**. JunB promotes ALCL development through transcriptional regulation of PDGF-Rß **(Laimer et al., 2012)**. Since PDGF-Rß is not expressed in the human SR-786 cell line, murine ALCL CD-417 cells were used to test the impact of Neurolenin B on PDGF-Rß expression. The inhibition of NPM/ALK expression (after 4 h) was followed by the inhibition of JunB and PDGF-Rβ (**Fig. 17b**) according to the recently discovered NPM/ALK signal transduction cascade **(Laimer et al., 2012)**.

Although Neurolenin A inhibited the expression of NPM/ALK, but also that of c-Jun and p21 in SR-786 cells after 24 h, this may have been the reason why Neurolenin A did not attenuate the proliferation of ALCL cells. Furthermore, this indicated that Neurolenin A treatment (for 24 h) disconnected JunB from the direct control by NPM/ALK.

a b

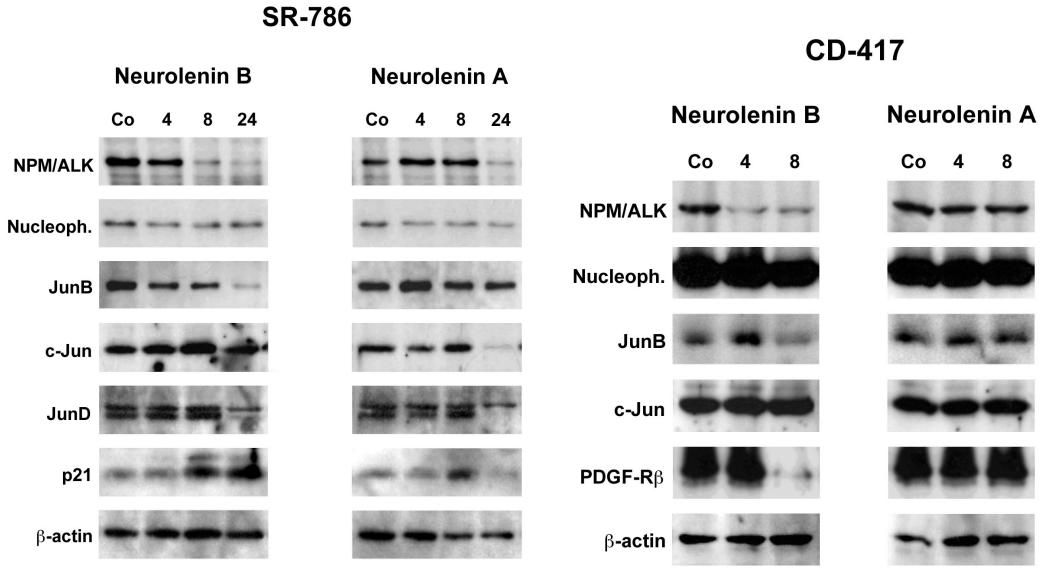

Figure 17. Protein expression analysis upon Neurolenin A and B treatment in SR-786 (a) and CD-417 (b) cells. Both cell lines received 3 µM Neurolenin A and B treatment. After 4 h, 8 h and 24 h of incubation cells were harvested and subjected to Western blot analysis using the indicated antibodies. β-actin expression served as control for equal sample loading.

Neurolenin B decreases the NPM/ALK transcript level

To elucidate at which stage NPM/ALK was regulated by Neurolenin B, the mRNA level was measured in SR-786 cells. Neurolenin B decreased NPM/ALK transcripts and also JunB mRNA consistent with the findings reported earlier **(Laimer et al., 2012; Staber et al., 2007)**. Interestingly, Neurolenin B induced rather than inhibited the mRNA expression of nucleophosmin indicating that the 5´part of the nucleophosmin genomic sequence was not a target of Neurolenin B.

a b c

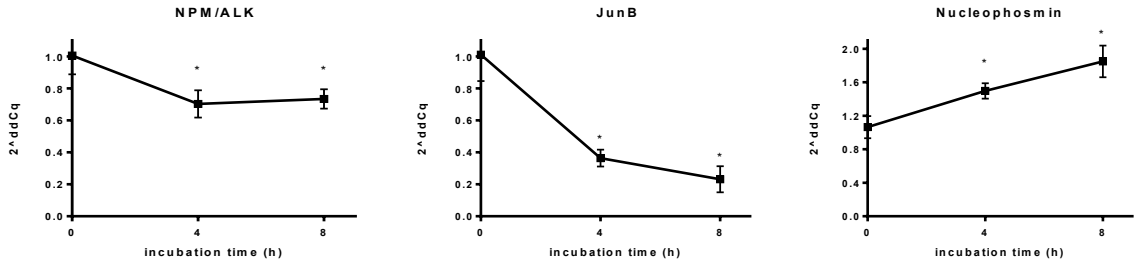

Figure 18.Quantitative PCR analysis of NPM-ALK (a), JunB (b) and nucleophosmin (c) mRNA expression in SR-786 normalized to GAPDH mRNA. Experiments were performed in triplicate, error bars indicate means +/- SD, and asterisks significance ($p<0.05$; t-test).

Apoptotic and necrotic effects of Neurolenin B

In order to examine whether Neurolenin B induced cell death, Western blot analysis detecting caspase 3 activation was performed (**Fig. 19a**). After 24 h of Neurolenin B treatment caspase 3 became cleaved and PARP signature-type degraded, whereas PARP and caspase 3 remained unaffected upon Neurolenin A treatment. An independent assay monitoring caspase 3/7 activity confirmed the Western blot data (**Fig. 19b**). Neurolenin B treatment led to an extremely elevated caspase 3/7 activity within 16 h that persisted. Cell death results were supported by HO/PI double staining. Neurolenin B treatment induced cell death, whereby significantly more apoptotic than necrotic cells were counted (**Fig. 19c**).

a

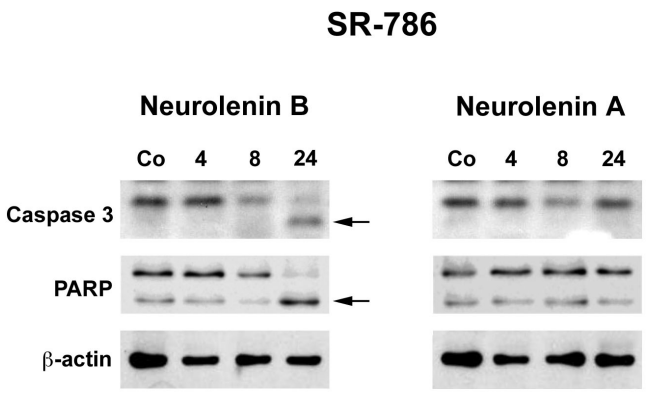

b

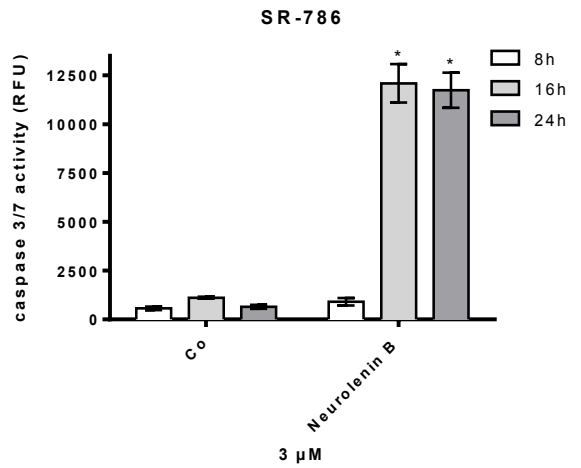

c

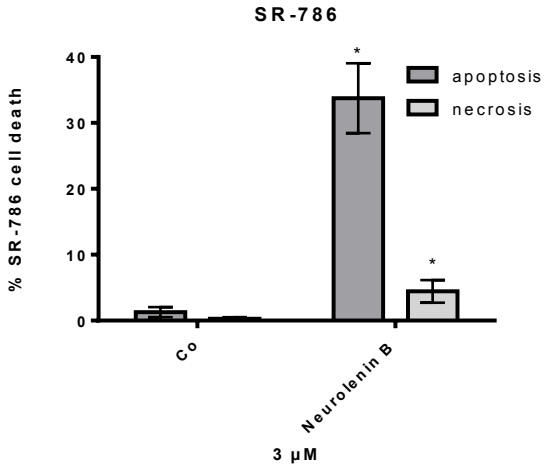

Figure 19. Apoptotic and necrotic effects in Neurolenin B treated SR-786 cells. (a) SR-786 were treated with 3µM Neurolenin A and B for 4h , 8h and 24h, harvested and subjected to Western blot analysis. β-actin expression served as control for equal sample loading. (b) ApoOne reagent was added to 3 µM Neurolenin B treated cells after 8 h, 16 h and 24 h and then, caspase3/7 activity was measured. (c) Cells were treated with 3 µM Neurolenin B and after 24 h PI and Hoechst 33258 (HO/PI) was added. Experiments were performed in triplicate, error bars indicate means +/- SD, and asterisks significance ($p<0.05$; t-test)

Impact of Neurolenin B on NPM/ALK negative cell types

Neither Neurolenin A nor Neurolenin B treatment decreased PBMC numbers (**Fig. 20a**). Interestingly, the mitochondrial activity increased upon treatment with Neurolenin B for 8 h (**Fig. 20b**) but returned to control levels thereafter. In contrast, the HL60 cell number decreased upon Neurolenin B treatment (**Fig. 20a**) and also the mitochondrial activity of HL60 cells was significantly reduced after 24 h (**Fig. 20b**). Thus, also leukaemia cells, which are not harbouring the NPM/ALK translocation, were affected by an as yet unknown mechanism of Neurolenin B. Also Lobatin B was shown to inhibit HL60 cell proliferation, which was attributed to the inhibition of NF-κB activity. Therefore, Neurolenin B exhibited anti-leukaemia/lymphoma specificity leaving normal blood cells unaffected.

a

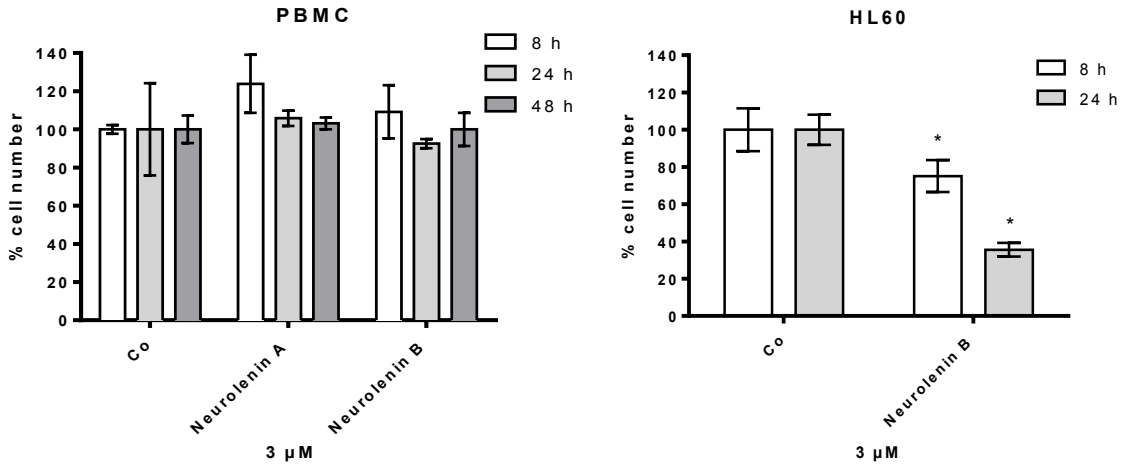

b

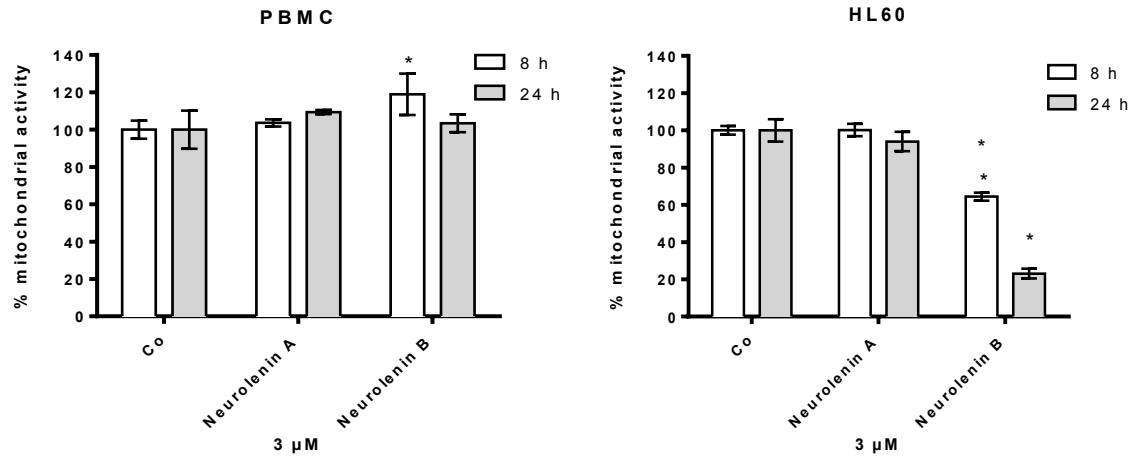

Figure 20. Effects of Neurolenin A and B treatment on PBMC and HL60 mitochondrial activity and cell number. (a) Anti-proliferative effects of 3 µM Neurolenin A and B in PBMCs and HL60 cells were evaluated. After 8 h, 24 h and 48 h of treatment cells were counted using a Casy cell counter. The relative cell number is presented as percent of control. (b) PBMCs and HL60 cells were treated with 3 µM Neurolenin A and B, and after 8 h and 24 h of incubation CellTiter-Blue reagent was added and measured at 570 nm. Experiments were performed in triplicate, error bars indicate means +/- SD, and asterisks significance ($p<0.05$; t-test).

Effects of the specific ALK inhibitor TAE-684 in CD-417 cells

To test whether a specific ALK inhibitor performs similar to Neurolenin B, CD-417 cells were treated with TAE-684 and protein expression was investigated. 10 nM TAE-684 inhibited significantly the proliferation of CD-417 cells after 24 h but induced cell growth within 8 h (**Fig. 21a**), which was also observed for Neurolenin C and D (**Fig. 15**). NPM/ALK was down-regulated by TAE-684 treatment and consequently JunB expression became inhibited after 4 h and PDGF-Rß suppressed after 24 h (**Fig. 21b**). The NPM/ALK protein level remained unaffected, because TAE-684 interferes with the phosphorylation of ALK and therefore, inhibits its activity but not its expression (**Fig. 21b**).

a

b

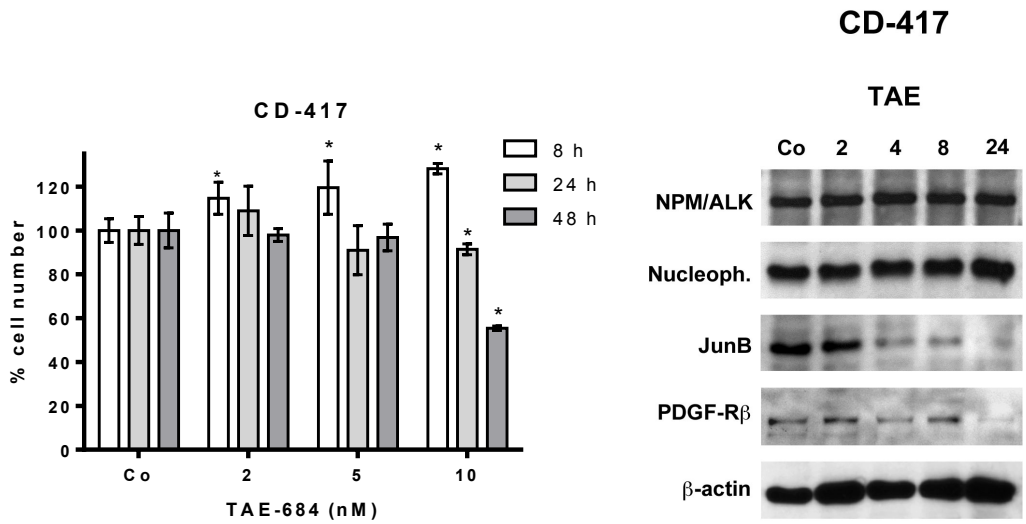

Figure 21. Effects of the specific ALK-inhibitor TAE-684. (a) CD-417 cells were treated with the indicated TAE-684 concentrations for 8 h, 24 h and 48 h and then counted using Casy cell counter. The relative cell number is presented as percent of control. Experiments were performed in triplicate, error bars indicate means +/- SD, and asterisks significance ($p<0.05$; t-test). (b) Western blot analysis CD-417 protein extracts upon treatment with TAE-684. Cells were treated with 10 nM TAE-684 for 2 h, 4 h, 8 h and 24 h, then harvested and subjected to Western blot analysis using the indicated antibodies. Equal sample loading was checked by ß-actin expression.

DISCUSSION

The focus of this research was on seeking a new promising therapy for NPM/ALK positive ALCLs. The isolated *furanoheliangolide* and *germacranolide* sesquiterpene lactones of the traditional healing plant *N. lobata* were tested regarding their antineoplastic properties. Thereby, Neurolenin B belonging to the *germacranolides* and Lobatin B from the *furanoheliangolides,* were identified as the most active compounds among the eight isolated and tested sesquiterpene lactones. Former studies have presented sesquiterpene lactones as effective constituents against human cancer and tumour cell lines such as A2780, A431, HeLa, MCF7, GLC4 and COLO 320 **(Lajter et al., 2014; Francois et al., 1996)**.

Both compounds, Neurolenin B and Lobatin B, exhibited similar properties particularly with respect to anti-proliferative, mitochondrial- and cell cycle activities, but also similar anti-inflammatory properties **(McKinnon et al., 2014; Walshe-Roussel et al., 2013)**.

Moreover, Neurolenin B and Lobatin B caused a downregulation of the oncogene NPM/ALK due to transcript level decrease. Such a suppression of NPM/ALK caused by *N. lobata* DME (dichloromethane extract) was reported earlier **(Unger et al., 2013)** and resulted in apoptosis of ALCL cells. Unlike Neurolenin B, Lobatin B reduced not only NPM/ALK but also non-truncated nucleophosmin transcript level. Hence, it can be assumed that the responsible transcription mechanism for nucleophosmin, the fusion partner of the NPM/ALK t(2;5)(p23;q35) translocation, was obstructed. As a consequence of NPM/ALK downregulation by Neurolenin B and Lobatin B, JunB and PDGF-Rβ became subsequently inhibited. These observations are in agreement with **Laimer et al. (2012)** who report that NPM/ALK induces JunB and in succession, malignancies are expedited via transcriptional activation of PDGF-Rβ.

Pleiotropic effects are also noticed for Lobatin B, whereby Lobatin B seemed to be more potent and thus, the inhibition cascade occurred faster than by Neurolenin B treatment.

Furthermore, Neurolenin B and Lobatin B caused a decrease of G1-phase cells and an accumulation of cells in G2/M-phase most likely by an upregulation of p21. Induced as well as suppressed c-Jun levels were reported to cause p21-mediated G2/M arrest in ALK positive ALCL **(Kardassis et al., 1999; Leventaki et al., 2007)**. The upregulation of c-Jun by Lobatin B and also by the DME of *N. lobata* **(Unger et al., 2013)** was similar to the enhanced c-Jun level by Neurolenin B but the regulation of c-Jun itself is still unclear.

However, even the inactive *germacranolide* Neurolenin A inhibited NPM/ALK expression with a slight downregulation of JunB but this was insufficient to induce p21 expression and to arrest the cell cycle. Also the inactive *furanoheliangolide* OH-CAL was shown to downregulate JunB temporarily but independent from NPM/ALK. OH-CAL treatment caused also minor pre-activation of caspase 3 but this did not affect the viability of SR-786 cells.

Additionally, TAE-684, a specific ALK-inhibitor, which inhibits phosphorylation of NPM/ALK and its downstream effectors thereby promoting apoptosis and cell cycle arrest of ALK+ ALCL cells **(Galkin et al., 2007)**, was tested.

TAE-684 was more specific in targeting ALK than Neurolenin B or Lobatin B, because both sesquiterpenes affected the proliferation of ALK-negative HL60 cells, whereas TAE-684 did not intimidate HL60 growth. Thus, the anti-neoplastic effects of Neurolenin B or Lobatin B were not restricted to NPM/ALK-positive cells and this was most likely due to additional properties of these compounds, which specifically target NF-kB.

Altogether, our investigations indicated that cancer cells are targets of Neurolenin B and Lobatin B and healthy cells, such as PBMCs, are not affected by Neurolenin B and Lobatin B probably due to the fact that these cells do not depend on NF-kB-signalling. Neurolenin B and Lobatin B did not rigorously disturb mitochondrial activity of SR-786 cells and cell death was triggered by more specific mechanisms i.e. the inhibition of NF-kB- or NPM/ALK - JunB- dependent survival signals.

Both compounds, Neurolenin B and Lobatin B, exhibited features that make the compounds interesting for developing new efficient therapies with less side effects for ALCL and other tumours relying on NF-kB signalling. But before the sesquiterpene lactones are considered as a therapy for NPM/ALK+ ALCLs further investigations have to be conducted to study the specific regulation of NPM/ALK by these sesquiterpene lactones.

MATERIAL AND METHODS

Cell culture

SR-786 NPM-ALK positive human ALCL (anaplastic large cell lymphoma) cells were from DSMZ (Braunschweig, Germany), CD-417 NPM-ALK positive mouse ALCL cells were isolated from *CD4*-NPM-ALK mice, HL60 (human promyelocytic leukemia cells) were from ATCC (Manassas, VA, USA). PBMC (peripheral blood mononuclear cells) were isolated from peripheral blood. All cells were grown in RPMI 1640 medium (Life Technologies, Carlsbad, California, USA) supplemented with 10 % heat inactivated FCS (Heat Inactivated Fetal Calf Serum, Life Technologies, Carlsbad, California, USA), 1 % L-Glutamine (Lonza, Verviers, Belgium) and 1 % antibiotics (Penicillin/Streptomycin, Sigma-Aldrich, St. Louis, MO, USA) and maintained in humidified atmosphere containing 5% CO_2 at 37°C.

N. lobata compounds

All compounds were dissolved and prepared in DMSO (Sigma-Aldrich, St. Louis, MO, USA) as concentrated stock solutions, and stored at -20°C. Controls were treated with the respective concentrations of DMSO used in sample treatment. In order to avoid cell damage due to DMSO toxicity the maximum final concentration was limited to 0.5%.

PBMC isolation

Peripheral blood mononuclear PBMC cells were isolated from human peripheral blood by density-gradient centrifugation. 50 ml blood was collected by using a heparin (anticoagulants, Sigma-Aldrich, St. Louis, MO, USA) coated syringe. Then, blood was diluted with an equal volume of PBS (1x DPBS, Lonza, Verviers, Belgium) and afterwards two parts of diluted cell suspension was carefully laid over one part Ficoll-Paque Plus (hydrophilic polysaccharide that separates layers of blood, GE Healthcare, Little Chalfont, United Kingdom) in a conical tube. A centrifuge step followed at 400 x g for 35 min at room temperature (RT) without break. The upper layer (Plasma) was aspirated by leaving the white cell layer (mononuclear cell layer-PBMC) undisturbed at the interface. PBMCs were transferred to a new tube by trying to retrieve all cells from the interface without disturbing the red pellet (erythrocytes) at the bottom of the Ficoll layer. Then, an equal volume of PBS was added to wash PBMCs. Cells were gently mixed and centrifuged at 300 x g for 7 min at RT. The supernatant was discarded and the pellet was resuspended in PBS and centrifuged at the same conditions as before. To increase purity two further washing steps were performed at 200 x g. Finally, cells were resuspended in culture media. All steps were performed at RT.

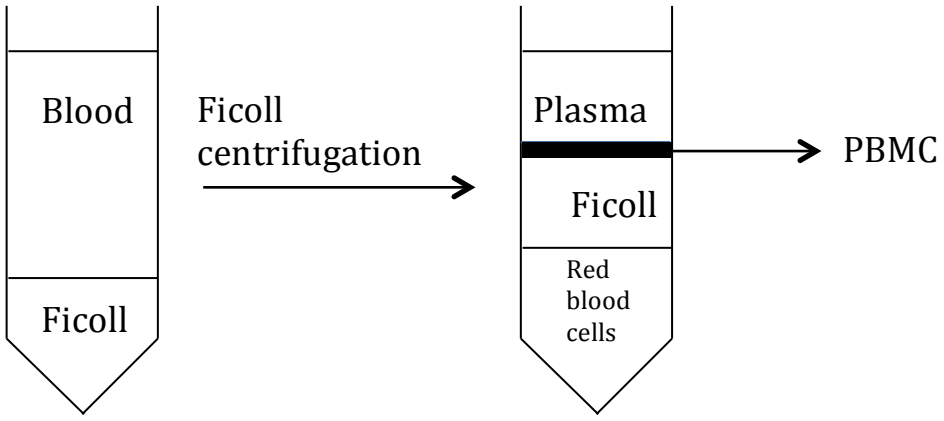

Proliferation assay (SR-786, CD4-417, PBMC, HL60)

To determine which compounds of *N. lobata* inhibit proliferation, SR-786, CD-417, PBMC and HL-60 were first counted by using a Casy cell counter (Roche Innovatis AG, Bielefeld, Germany). All cell lines were seeded in a 24-well plate, SR-786 at a concentration of 2 x 10^5 cells/ml, CD-417 cells at a concentration of 1 x 10^6 cells/ml, PBMC at a concentration of 5 x 10^5 and HL60 cells at a concentration of 1 x 10^5 cells/ml. Then, cells were incubated with 1 µM and/or 3 µM of the compounds for 4, 8, 16 and 24 h. PBMC were treated with the indicated concentration just for 8, 16 and 24 h. All experiments were carried out in quadruplicate.

Western blotting

Lysate preparation

SR-786 and CD-417 cells were counted by using Casy cell counter and seeded in 6 cm dishes. SR-786 cells were seeded at a concentration of 2 x 10^5 cells/ml and CD-417 at a concentration of 10^6 cells/ml. After treating cells with 3 µM of *N. lobata* compounds for the indicated times they harvested. As controls served samples harvested at the beginning of cell treatment.

All cells were centrifuged at 1000 rpm for 5 min at 4°C and washed twice with cold PBS. Supernatant was discarded and the cell pellet lysed in RIPA buffer (150 mM NaCl, 50 mM, Tris pH 7,6, 1 % Triton, 0,1 % SDS, 0,5% Sodium deoxycholate) containing 1 mM phenylmethylsulfonyl (PSMF, Sigma-Aldrich, St. Louis, MO, USA) and 1 mM protease inhibitor mixture (PIM consists of 2µg/ml Leupeptin, 2µg/ml Aprotinin, 0,3 µg/ml Benzamidine chloride and 10µg/ml Trypsin inhibitor, Sigma-Aldrich, St. Louis, MO, USA) followed by an short incubation time of 5 min on ice. Lysates were centrifuged at 12000 rpm for 20 min at 4°C. Supernatant was transferred into an Eppendorf tube and stored at -20°C until further analysis.

Protein quantification

Protein concentration was determined by Bradford assay (Protein Assay Dye reagent Concentrate, BioRad, Hercules, CA, USA). To measure the protein concentration, 1 µl of sample was added to 500 µl Bradford solution in a cuvette and resuspended followed by 5 min of incubation. Concentration was measured at 595 nm by using a Bio-Photometer (Eppendorf, Hamburg, Germany).

Polyacrylamid Gel Electrophoresis (SDS-PAGE)

Equal amounts of lysates were mixed with SDS (sodium dodecyl sulfate, Sigma-Aldrich, St. Louis, MO, USA) sample buffer (4x SDS sample buffer: 200mM Tris pH 6,8; 400mM DTT (Dithiothreitol, Sigma-Aldrich, St. Louis, MO, USA); 8% SDS; 0,4% Bromphenolblau (Merck, Darmstadt, Germany); 40% Glycine (Sigma-Aldrich, St. Louis, MO, USA)), denatured at 95°C for 5 min and loaded onto a polyacrylamide gel (30 % Acrylamide/Bis-Acrylamide Solution, Sigma-Aldrich, St. Louis, MO, USA), consisting of a stacking (Buffer pH8,8: 1,5M Tris; 0,4% SDS, APS, TEMED, acrylamide) and a 11.5% separation gel (Buffer pH6,8: 0,5M Tris; 0,4% SDS, APS, TEMED, acrylamide). First, samples were concentrated through the stacking gel at 70 Volt and when the samples formed a straight line the voltage was increased to 110V to separate proteins.

Western blotting

Proteins were electro-transferred from the gel onto a nitrocellulose membrane (Watman, Dassel, Germany) at 350 mA for 1 h. Equal sample loading was checked by staining the membrane with 1x Ponceau S (10% (v/v) 10x Ponceau S: 2% (w/v) Ponceau S, 30% (w/v) trichlor acetic acid, 30% (w/v) sulfosalicylic acid, Sigma-Aldrich, St. Louis, MO, USA) for 10 min.

Protein detection

After a short washing step with 1x Tris buffered saline pH 7,4 (10x TBS consists of 1,5 M NaCl and 0,5M Tris/HCl, (Trisma Base, Sigma-Aldrich, St. Louis, MO, USA)) containing 0.1 % Tween 20 (BioRad, Hercules, CA, USA, 170-6531), free and non-specific binding sites were blocked by incubating the membranes in TBS/T-milk (5 % Fixmilk instant, Maresi, Vienna, Austria) at RT for 1 h. Membranes were washed three times with TBS/T for 30 min each. Then, membranes were incubated with a primary antibody in TBS/T- bovine serum albumin (5% BSA Fraction V, GE Healthcare, Little Chalfont, United Kingdom) diluted 1:200 – 1:10 000 by agitating them gently at 4°C over night. Next, membranes were washed with TBS/T and incubated with the second antibody (peroxidase conjugated goat anti-rabbit IgG or anti-mouse IgG, Invitrogen, Carlsbad, CA, USA) diluted 1:10 000 in TBS-milk at RT for 1 h. Chemiluminescence was developed by ECL detection kit (Thermo Scientific, Waltham, MA, USA) and membranes were exposed to Amersham Hyperfilms (GE Healthcare, Buckinghamshire, UK) and CL-XPosure films (Thermo Scientific, Rockford, IL, USA).

Stripping

In order to apply new antibodies the former antibodies were stripped off the membrane. For this, membranes were placed in 75 ml stripping buffer (4,5 ml 1M Tris-HCL pH 6,4; 7,5 ml 20% SDS; 0,5 ml beta-Mercapthoenthanol, add dH_2O up to 75ml) for 6-15 min shaking in a 55°C water bath and afterwards membrane was washed until no beta-mercaptoethanol (2-Mercaptoethanol, min. 98 %, Merck, Darmstadt, Germany) smell was recognized. Then, free non-specific binding sites were blocked by agitating membranes in TBS/T-milk at RT for 1 h. Membranes were washed with TBS/T changing washing solution three times within 30 min.

Antibodies

CD246, ALK protein, monoclonal mouse, clone ALK1, code M7195 (DakoCytomation, Glostrup, Denmark)

Nucleophosmin, monoclonal mouse, clone 376, code M7305 (DakoCytomation, Glostrup, Denmark)

PDGF Receptor β (28E1) Rabbit mAB, #3169 (Cell Signaling, Cambridge, UK)

PARP-1 (F-2): sc-8007, mouse monoclonal (Santa Cruz Biotechnology, Inc., Santa Cruz, CA, USA)

Cleaved Caspase3 (Asp175) Antibody, #9661 (Cell Signaling, Cambridge, UK)

JunB (120): sc-73, rabbit polyclonal (Santa Cruz Biotechnology, Inc. Santa Cruz, CA, USA)

JunD(329):sc-74, rabbit polyclonal (Santa Cruz Biotechnology, Inc. Santa Cruz, CA, USA)

c-Jun (H-79): sc-1694, rabbit polyclonal (Santa Cruz Biotechnology, Inc. Santa Cruz, CA, USA)

p21 (C-19): sc-397, rabbit polyclonal (Santa Cruz Biotechnology, Inc. Santa Cruz, CA, USA)

ß-actin: monoclonal mouse ascites fluid, clone AC-15, Cat. No. A5441 (Sigma, St. Louis, MO, USA)

Quantitative RT-PCR

RNA preparation

SR-786 cells were seeded in a 24 well at a concentration of 2 x 10^5 cells/ml and incubated for some hours before treating them with 3 µM of *N. lobata* compounds. After 1, 2, 4 and 8 h cells were harvested, washed twice with cold PBS and centrifuged at 800 rpm for 5 min at 4°C. As control a sample was taken at the beginning of the experiments before the compounds were added.

For RNA preparation ReliaPrep™ RNA Cell Miniprep System Kit (Promega, Madison, WI) was used. Each Cell pellet was resuspended in 100 µL BL+TG Buffer (4M Guanidine thiocyanate 0.01M Tris (pH 7.5), 2% 1-Thioglycerol) and stored at -80°C until further processing. 35 µL 100% isopropanol was added to each sample and mixed for 5 sec.

Next, ReliaPrep™ minicolumns were placed into collection tubes, lysates were transferred to the columns and centrifuged at 13 000 x g for 30 sec at RT. The flow–through was discarded, 500 µL RNA wash solution (62.8mM potassium acetate, 27.1mM Tris-HCl (pH 7.5 at 25°C), after dilution with ethanol the final concentration (approximate) is 60mM potassium acetate, 10mM Tris-HCl (pH 7.5 at 25°C) and 60% ethanol) was added to the columns and centrifuged at 13000 x g for 30 sec. During this centrifugation step, DNase I incubation mix was prepared by combining the following amount of each reagent per sample: Freshly prepared DNase I incubation mix consisting of 24 µl Yellow Core Buffer (0.0225M Tris (pH 7.5) 1.125M NaCl, 0.0025% yellow dye (w/v) 3 µl 90 mM $MnCl_2$ and 3 µl DNase I enzyme was directly pipetted onto the membrane inside the column and incubated for 15 min at RT. Then, 200 µl of Column Wash Solution (before use 95% ethanol was added to concentrated Column wash solution) was added to the mini-column and centrifuged at 13 000 × *g* for 15 sec.

Next, 500 µL RNA Wash Solution was added, followed by a 13 000 x *g* centrifugation step for 30 sec and a second washing step using 300 µl RNA Wash Solution followed by high speed centrifugation for 2 min. Finally, mini-columns were placed in an Eppendorf tube, and samples eluted with 20 µL nuclease-free water and centrifuged at 13 000 × g for 1 min. The concentration of the purified RNA was measured by using a NanoDrop Fluorospectrometer (Thermo Fisher Scientific, Waltham, MA, USA) and stored at -80°C until further use. The entire procedure was performed on ice.

cDNA synthesis

First-strand cDNA synthesis was carried out with 150 ng RNA by using GoScript™ Reverse Transcription System Kit (Promega, Madison, WI). cDNA synthesis reaction was primed by using Oligo(dT)$_{15}$ (0.5µg/reaction). Samples were heated at 70°C in a heat block for 5 min. During a 5 min incubation time on ice, the reverse transcription reaction mix was prepared adding first 7,3 µl Nuclease-free water, 4 µl GoScript™ 5x Reaction buffer, 1,2 µl $MgCl_2$, 1 µl PCR Nucleotide mix, 0,5 µl Recombinant RNasin® Ribonuclease Inhibitior and at least 1 µl GoScript™ Reverse Transcriptase.

One sample was prepared without reverse transcriptase enzyme to serve as contamination control.

15 µL reverse transcription reaction mix was added to each first strand cDNA template, annealing was performed at 25°C for 5 min and extension samples at 42°C for up to 1 h. Finally, before proceeding with qPCR the reverse transcriptase was inactivated by heating samples to 70°C for 15 min. The cDNA was stored at -20°C for further use.

Real time-PCR

The expression of NPM-ALK, JunB and NPM transcript levels in SR-786 cells after treatment with active *N. lobata* compounds was examined by real-time PCR (Polymerase chain reaction) using SYBR Green detection system (Promega, Madison, WI). The housekeeping-gene GAPDH (glyceralaldehyde 3-phosphat dehydrogenase), which is stably and constitutively expressed at high levels in most tissues and cells, served as reference gene for qPCR normalization. For each sample, 10 µl GoTaq qPCR Master Mix (are premixed solutions containing GoTaq® DNA Polymerase, GoTaq® Reaction Buffer, dNTPs and Mg2+, Promega, Madison, WI) 2 µl forward primer and 2 µl reverse primer (see sequences below), 5 µl nuclease free water and 1 µl cDNA, were added to the wells of a 96-well optical reaction plate. Real time-PCR was carried out in quadruplicate for each cDNA template, Water instead of cDNA served as negative control. The cycle program was: 50°C for 2 min, 95°C for 10 min to activate polymerase, 40 cycles of 95°C for 15 sec and 60°C for 1 min. (Thermocycler Primus25 advanced, Peqlab, Erlangen, Germany).

Used primers for RT-PCR are listed below.

GAPDH	fw: 5´- AACAGCGACACCCACTCCTC -3´ rev: 5´- CATACCAGGAAATGAGCTTGACAA -3´
NPM/ALK	fw: 5´-GTG GTC TTA AGG TTG AAG TGT GGT T-3´ rev: 5´-GCT TCC GGC GGT ACA CTA CTA A-3´
Nucleophosmin	fw: 5´-TCCCTTGGGGGCTTTGAAATAACACC-3´ rev: 5´-TGGAACCTTGCTACCACCTC-3´
JunB	fw: 5´-GCTCGGTTTCAGGAGTTTGT-3´ rev: 5´-ATACACAGCTACGGGATACGG-3´

Analysis of results

To analyse qPCR data, comparative C_t ($\Delta\Delta C_t$) method **(Livak and Schmittgen, 2001)** for relative quantification of gene expression was used. The threshold cycle (C_t) is defined by the number of cycles at which the fluorescence exceeds the threshold. To quantify relative expression of the target genes NPM/ALK, Nucleophosmin and JunB following formula was used:

ΔCT = CT target gene (NPM/ALK, Nucleophosmin, JunB) – $\bar{x}$ CT control gene (GAPDH)

ΔΔCT = ΔCT drug treatment – $\bar{x}$ ΔCT control sample

Ratio = 2-ΔΔCT

Cell cycle progression (FACS-analysis; performed by the group of Michael Grusch)

SR-786 cells were seeded in a 6-well plate at a concentration of 2 x 10^5 cells/ml followed by a short incubation time of 1h at 37°C. Concentrated stock solutions of *N. lobata* compounds were diluted in PBS before they were added to the cells at a final concentration of 3 µM. After 8 and 24 h of incubation at 37°C, cells were harvested and centrifuged at 800 rpm for 5 min at 4°C. Supernatants were discarded, cell pellets washed with cold PBS and centrifuged at 800 rpm for 5 min at 4°C. Pellets were resuspended in 1 ml cold 80% ethanol, and either fixed for 30 min at 4°C or stored at -20°C until further handling. After two washing steps with cold PBS (centrifugations at 600 rpm) supernatants were removed, cell pellets resuspended in 500 µl cold PBS, and transferred into a 5 ml polystyrene round bottom tube. Next, to each sample RNAse A and propidium iodide were added to a final concentration of 50 µg/ml and incubated for 2h at 4°C, whereby the final cell number was adjusted to 0.5 and 1 x 10^6 cells in 500 µl. Cells were analysed by FACS Calibur flow cytometer (BD Bioscience, Franklin Lakes, New Jersey, USA). Experiments were performed in triplicate.

Cytotoxicity, mitochondrial activity assay

To evaluate mitochondrial activity and cytotoxicity, CellTiter-Blue assay (Promega, Madison, WI) was applied. The CellTiter-Blue assay is based on the ability to convert the blue non-fluorescent resazurin, a non-toxic and cell permeable dye, into red fluorescent resorufin. The produced amount of fluorescence corresponds to metabolic active cells and thus, the fluorescent signal increases proportional with the number of intact cells. Compromised cells gradually lose their metabolic capacity to convert the indicator dye.

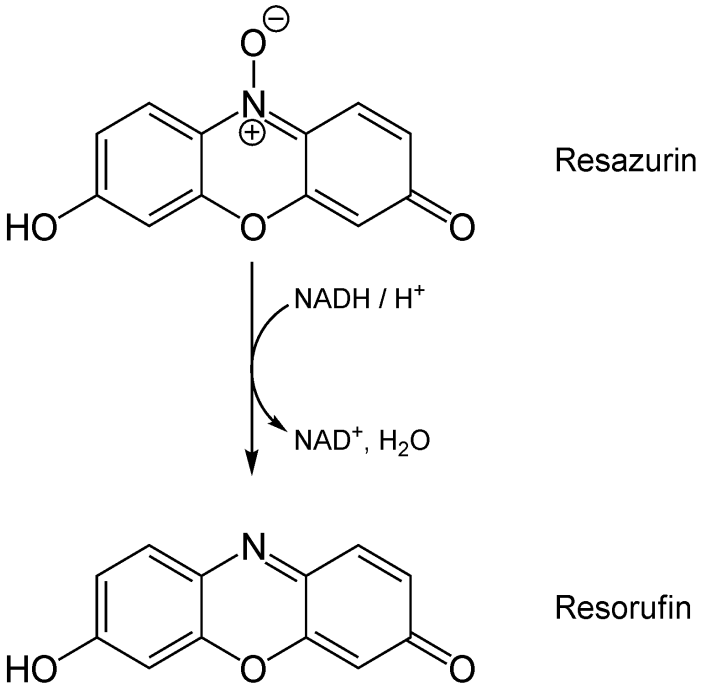

Figure 22. Non-fluorescent resazurin is converted into flourescent resofurin by reduction in cell metabolism. **(Taken from http://de.wikipedia.org/wiki/Resazurin)**

SR-786, PBMC and HL60 cells were seeded into 96-well plates at concentrations of 2 x 10^5, 5 x 10^5 and 1 x 10^5cells/ml, respectively, and each well was filled up to 250 µl with the cell suspensions. *N. lobata* compounds were added at a concentration of 3 µM and TAE-684 was added at a concentration of 10ng/ml and compared to solvent-treated controls. After 8 h and 24 h 25 µl CellTiter- Blue reagent was added to each well and incubated for 120 minutes at 37°C until the colour changed from blue to pink.

Afterwards, the 96-well plates were placed into a multi-detection reader to measure fluorescence at 570 nm (Synergy HT, Bio-Tek Instrument, Winooski, VT, USA). Experiments were done in quadruplicate. To eliminate possible background fluorescence of the medium, the mean blank value consisting of medium and CellTiter-Blue reagent was subtracted from all other measured values. The mitochondrial metabolic activity of the untreated control cells was set as 100 %. All experiments were performed with an active and an inactive compound of *N. lobata* and with the ALK-inhibitor TAE-684 (Selleckchem, Houston, TX, USA).

Apoptosis assay – (HOPI staining)

Hoechst 33258 (HO) and propidium iodide (PI) double staining (Sigma-Aldrich, St. Louis, MO, USA) allows the determination of the cell death type, apoptosis or necrosis **(Grusch et al., 2002)**. SR-786 cells were seeded in a 96-well flat bottom plate at concentrations of 2 x 10^5 cells/ml. Each well contained 100 µL cell-suspension and treated with a concentration of 3 µM N. lobata compounds. After 24 h of incubation Hoechst 33285 and propidium iodide were added at final concentrations of 50 µg/ml and 20 µg/ml. After 1 h of incubation at 37°C, stained cells were photographed using a fluorescence microscope (Olympus IX51, Shinjuku, Tokio, Japan). The fluorescence microscope was equipped with a TRITC and DAPI filter. Photographs were visually examined to count the cell number and type of cell death (necrosis or apoptosis). Experiments were performed in quadruplicate.

Caspase 3/7 activity assay

In principle, the Apo-ONE Homogeneous Caspase-3/7 Assay (Promega, Madison, WI) is based on a profluorescent substrate named rhodamine 110 bis-(N-CBZ-l-aspartyl-l-glutamyl-l-valyl-aspartic acid amide) (Z-DEVD-R110) and a cell lysis/activity buffer. The DEVD peptide is removed from rhodamine by increased caspase-3/7 activity and thus, rhodamine becomes fluorescent.

The excitation is at 499 nm and the emission maximum at 521 nm. The amount of generated fluorescence product is indicative for the amount of active caspase-3/7 present sample.

SR-786 cells were seeded in a 3.5 cm dish at a concentration of 2 x 10^5 cell/ml and after a short incubation of 1h at 37°C, cells were treated with 3 µg/ml of *N. lobata* compound. After 8, 16 and 24 h 25 µL of the treated cell suspension and 25 µL of untreated control were transferred into a 96-well plate. 25 µL of the substrate buffer solution (10µl Caspase Substrate Z-DEVD-R110 (100X) added to 1ml Apo-ONE® Homogeneous Caspase-3/7 Buffer) was added to each well. The plate was agitated (300 rpm) on a shaker for 30 minutes at RT and then, fluorescence was measured by using a multi-detection reader. Experiments were performed in triplicate.

Statistical analysis

For statistical analyses Excel 2003 software and Prism 5 software package (GraphPad, San Diego, CA, USA) were used. The values were expressed as mean ± SD and the Student's t-test was used to compare differences between controls and individual samples. Statistical significance level was set to $p < 0.05$.

REFERENCES

Bedoya LM, Alvarez A, Bermejo M, González N, Beltrán M, Sánchez-Palomino S, Cruz SM, Gaitán I, del Olmo E, Escarcena R, García PA, Cáceres A, San Feliciano A and Alcamí J (2008) Guatemalan plants extracts as virucides against HIV-1 infection. Phytomedicine 15: 520-524

Berger I, Passreiter CM, Ca´ceres A and Kubelka W1, (2001) Antiprotozoal Activity of Neurolaena lobata, PHYTOTHERAPY RESEARCH Phytother. Res. 15, 327–330
DOI: 10.1002/ptr.782

Bhanot A, Sharma R, Noolvi MN (2011) Natural sources as potential anti-cancer agents: A review, International Journal of Phytomedicine 3, 09-26

Chiarle R, Gong JZ, Guasparri I, Pesci A, Cai J, Liu J, Simmons WJ, Dhall G, Howes J, Piva R, Inghirami G. (2003) NPM-ALK transgenic mice spontaneously develop T-cell lymphomas and plasma cell tumors. Blood. 101(5):1919-1927

François G1, Passreiter CM, Woerdenbag HJ, Van Looveren M. (1996) Antiplasmodial activities and cytotoxic effects of aqueous extracts and sesquiterpene lactones from Neurolaena lobata. Planta Med., 62(2):126-9.

Galkin AV, Melnick JS, Kim S, Hood TL, Li N, Li L, Xia G, Steensma R, Chopiuk G, Jiang J, Wan Y, Ding P, Liu Y, Sun F, Schultz PG, Gray NS, Warmuth M. (2007) Identification of NVP-TAE684, a potent, selective, and efficacious inhibitor of NPM-ALK. Proc Natl Acad Sci U S A, 104(1): 270-5, Epub 2006 Dec 21

Gandhi, L. & Janne, P. A. (2012) Crizotinib for ALK-rearranged non-small cell lung cancer: a new targeted therapy for a new target. Clin Cancer Res 18, 3737-3742

Gidding CE, Kellie SJ, Kamps WA and de Graaf SS (1999) Vincristine revisited. Crit Rev Oncol Hematol 29: 267-287

Gordaliza M1, García PA, del Corral JM, Castro MA, Gómez-Zurita MA. (2004) Podophyllotoxin: distribution, sources, applications and new cytotoxic derivatives. Toxicon. 44(4): 441-59

Grusch M, Polgar D, Gfatter S, Leuhuber K, Huettenbrenner S, Leisser C, Fuhrmann G, Kassie F, Steinkellner H, Smid K, Peters GJ, Jayaram HN, Klepal W, Szekeres T, Knasmüller S and Krupitza G (2002) Maintenance of ATP favours apoptosis over necrosis triggered by benzamide riboside. Cell Death Differ 9: 169-178

Hallberg B1, Palmer RH. (2011) ALK and NSCLC: Targeted therapy with ALK inhibitors. F1000 Med Rep., 3:21, doi: 10.3410/M3-21, Epub 2011 Nov 1

Hanahan D, Weinberg RA, (2011) Hallmarks of Cancer: The Next Generation, Cell, Volume 144, Issue 5, Pages 646–674

Hande K.R (1998) Etoposide: four decades of development of a topoisomerase II inhibitor, Eur J Cancer. 34(10):1514-21

Johnson, I. S.; Armstrong, J. G.; Gorman, M.; Burnett, J. P. (1963) The Vinca Alkaloids: A New Class of Oncolytic Agents", Cancer Research 23 (8 Part 1): 1390–1427

Kadin, M.E. (1994) Ki-1/CD30+ (anaplastic) large-cell lymphoma: maturation of a clinicopathologic entity with prospects of effective therapy, J. Clin. Oncol. 12**,** 884–887

Kadin, M.E. (1994) Primary Ki-1-positive anaplastic large-cell lymphoma: a distinct clinicopathologic entity. *Ann.* Oncol. 5 (suppl. 1), 25–30

Kardassis D, Papakosta P, Pardali K, Moustakas A. (1999) c-Jun Transactivates the Promoter of the Human p21WAF1/Cip1 Gene by Acting as a Superactivator of the Ubiquitous Transcription Factor Sp1. J Biol Chem, 274, 29572-29581

Kiss I, Unger C, Kramer N, Atanasov A, Chi NH, Chatuphonprasert W, Brenner S, McKinnon-Popescu R, Peschel A, Kain R, Saiko P, Szekeres T, Kenner L, Hassler M, Diaz R, Frisch R, Dirsch VM, Jäger W, de Martin R, Bochkov V, Passreiter CM, Peter-Vörösmarty B, Mader RM, Grusch M, Dolznig H, Kopp B, Zupko I, Hohmann J, Krupitza G, Lobatin B inhibits NPM/ALK and NF-κB attenuating anaplastic-large-cell-lymphomagenesis and lymphendothelial tumour intavasation. Submitted

Laimer, D. et al. (2012) PDGFR blockade is a rational and effective therapy for NPM-ALK-driven lymphomas. Nat Med 18, 1699-1704

Lajter I, Vasas A, Béni Z, Forgo P, Binder M, Bochkov V, Zupkó I, Krupitza G, Frisch R, Kopp B, Hohmann J (2014) Sesquiterpenes from Neurolaena lobata and their antiproliferative and anti-inflammatory activities. J. Nat. Prod. 77(3): 576-82. doi: 10.1021/np400834c

Leventaki V1, Drakos E, Medeiros LJ, Lim MS, Elaenitoba-Johnson KS, Claret FX, Rassidakis GZ. (2007) NPM-ALK oncogenic kinase promotes cell-cycle progression through activation of JNK/cJun signaling in anaplastic large-cell lymphoma, Blood. 110(5): 1621-30

Livak KJ and Schmittgen TD (2001) Analysis of relative gene expression data using real-time quantitative PCRand the 2(-delta delta C(T)) method, Methods 25:402-408

Mathas S, Hinz M, Anagnostopoulos I, Krappmann D, Lietz A, Jundt F, Bommert K, Mechta-Grigoriou F, Stein H, Dörken B and Scheidereit C (2002) Aberrantly expressed c-Jun and JunB are a hallmark of Hodgkin lymphoma cells, stimulate proliferation and synergize with NF-kappa B. EMBO J 21: 4104-4113

McKinnon R, Binder M, Zupkó I, Afonyushkin T, Lajter I, Vasas A, de Martin R, Unger C, Dolznig H, Diaz R, Frisch R, Passreiter CM, Krupitza G, Hohmann J, Kopp B and Bochkov VN Pharmacological insight into the anti-inflammatory activity of sesquiterpene lactones from *Neurolaena lobata* (L.) R.Br. ex Cass. Running title: *Neurolaena lobata* compounds against inflammation. In print

Morris SW, Kirstein MN, Valentine MB, Dittmer KG, Shapiro DN, Saltman DL and Look AT (1994) Fusion of a kinase gene, ALK, to a nucleolar protein gene, NPM, in non-Hodgkin's lymphoma. Science 263: 1281-1284

Passreiter CM, Wendisch D and Gondol D (1995) Sesquiterpene lactones from *Neurolaena lobata.* Phytochemistry 39: 133-137

Passreiter et al., (1997) Antifeedant bioactivity of sesquiterpene Lactones from Neurolaena lobata and their Antagonism by gamma-Aminobutric Acid, Biochemical Systematics and ecology, Vol.25, No 5, pp. 371-377

Passreiter CM, (1998) Quantification of Sesquiterpene Lactones in Leaves of *Neurolaena lobata,* PHYTOCHEMICAL ANALYSIS, VOL. 9, 67–70

Pearson JD et al. (2011) NPM-ALK and the JunB transcription factor regulate the expression of cytotoxic molecules in ALK-positive, anaplastic large cell lymphoma, J Clin Exp Pathol. 4(2): 124-33

Pommier Y1, Leo E, Zhang H, Marchand C. (2010) DNA topoisomerases and their poisoning by anticancer and antibacterial drugs, Chem Biol. 17(5): 421-33. doi: 10.1016/j.chembiol.2010.04.012

Savage, K. J. et al. (2008) ALK- anaplastic large-cell lymphoma is clinically and immunophenotypically different from both ALK+ ALCL and peripheral T-cell lymphoma, not otherwise specified: report from the Internatinal Peripheral T-Cell Lymphoma Project, Blood 111, 5496-5504

Staber PB, Vesely P, Haq N, Ott RG, Funato K, Bambach I, Fuchs C, Schauer S, Linkesch W, Hrzenjak A, Dirks WG, Sexl V, Bergler H, Kadin ME, Sternberg DW, Kenner L, Hoefler G. (2007) The oncoprotein NPM-ALK of anaplastic large-cell lymphoma induces JUNB transcription via ERK1/2 and JunB translation via mTOR signaling. Blood, 110(9): 3374-83

Stein H. et al. (2000) CD30+ anaplastic large cell lymphoma: a review of its histopathologic, genetic, and clinical features. Blood 96, 3681–3695

Stein H. et al. (1985) The expression of the Hodgkin's disease associated antigen Ki-1 in reactive and neoplastic lymphoid tissue: evidence that Reed-Sternberg cells and histiocytic malignancies are derived from activated lymphoid cells, Blood, 66(4):848-58

Unger C, Popescu R, Giessrigl B, Laimer D, Heider S, Seelinger M, Diaz R, Wallnöfer B, Egger G, Hassler M, Knöfler M, Saleh L, Sahin E, Grusch M, Fritzer-Szekeres M, Dolznig H, Frisch R, Kenner L, Kopp B, Krupitza G (2013) The dichloromethane extract of the ethnomedicinal plant Neurolaena lobata inhibits NPM/ALK expression which is causal for anaplastic large cell lymphomagenesis. Int J Oncol. 42(1): 338-48

Walshe-Roussel B, Choueiri C, Saleem A, Asim M, Caal F, Cal V, Rojas MO, Pesek T, Durst T, Arnason JT (2013) Potent anti-inflammatory activity of sesquiterpene lactones from Neurolaena lobata (L.) R. Br. ex Cass., a Q'eqchi' Maya traditional medicine. Phytochemistry, 92:122-7

APPENDIX

Acknowledgements

First of all, I want to thank my supervisor **Prof. Dr. Georg Krupitza** for giving me the opportunity to work on such an interesting project and for his kind supervision, helpful advice and patience.

I am also very thankful to **Christine Unger** for her committed support during my diploma thesis and for sharing her experiences about the problem issues involved.

Special thanks are extended to all my **lab colleagues** and the **whole team of the Clinical Institute of Pathology** and the **Institute of Medical Genetics** for their helpfulness and for the great working atmosphere.

Last, but by no means least, I thank my family and friends who were always willing to lend me a sympathetic ear and help me regain perspective.

I am really grateful to all these people who supported and encouraged me throughout the entire process of writing this thesis.

Curriculum Vitae

PERSONAL INFORMATION

Name	Izabella Kiss
Nationality	Austria
Date of birth	[redacted]

EDUCATION

Since 10/2011	Master study of Molecular Biology at the University of Vienna Specialization in Molecular Medicine
10/2007-09/2011	Bachelor study of Biology at the University of Vienna Specialization in Microbiology and Genetics
09/2011	Degree: Bachelor of Science in Biology
09/1999-07/2007	BG/BRG St.Pölten, Josefstraße Graduation

WORK EXPERIENCE

06/2013-05/2014	**Master thesis** at the **Medical University,** Vienna
Department	Clinical Institute of Pathology/ Institute of Medical Genetics, Prof. Georg Krupitza
Thesis title	Bioactive compounds of *N. lobata* inhibit translocated NPM/ALK gene
Since 11/2011	**Tutor** at the **University of Vienna**
Courses	Laboratory courses in Microbiology and Molecular Biology
07/2011	**Bachelor thesis** at the **Max F. Perutz Laboratories**, Vienna
Department	Microbiology, Immunobiology and Genetics, Prof. Isabella Moll
Thesis title	Purification of stress-ribosomes and cell-free protein synthesis
06/2011	**Internship** at the **Böhm-Klein-Wonnerth** medicine-diagnostic Laboratory
Department	Microbiology
Since 03/2011	**Tutor** at the **Vienna Open Lab** Laboratory courses

Papers

Kiss I, Unger C, Atanasov A, Chi NH, Chatuphonprasert W, Brenner S, Kramer N, McKinnon-Popescu R, Peschel A, Kain R, Saiko P, Szekeres T, Kenner L, Hassler M, Diaz R, Frisch R, Dirsch VM, Jäger W, de Martin R, Bochkov V, Passreiter CM, Peter-Vörösmarty B, Mader RM, Grusch M, Dolznig H, Kopp B, Zupko I, Hohmann J, Krupitza G, Lobatin B inhibits NPM/ALK and NF-κB attenuating anaplastic-large-cell-lymphomagenesis and lymphendothelial tumour intavasation. Submitted

Unger C, Kiss I, Atanasov A, Chi NH, Chatuphonprasert W, Brenner S, McKinnon-Popescu R, Kramer N, Peschel A, Kain R, Saiko P, Szekeres T, Kenner L, Hassler M, Diaz R, Frisch R, Dirsch VM, Jäger W, de Martin R, Bochkov V, Passreiter CM, Peter-Vörösmarty B, Mader RM, Grusch M, Dolznig H, Kopp B, Zupko I, Hohmann J, Krupitza G, The germacranolide sesquiterpene lactone Neurolenin B of the healing plant *Neurolaena lobata* inhibits NPM/ALK-driven cell expansion and NF-kB-driven tumour intravasation. Submitted